Mechanisms Underlying Bone Cell Recovery During Zebrafish Fin Regeneration

by

Sumeet Pal Singh

University Program in Genetics and Genomics
Duke University

Date:_____

Approved:

_____
Kenneth Poss, Supervisor

_____
Blanche Capel, Chair

_____
Scott Soderling

_____
Michel Bagnat

Dissertation submitted in partial fulfillment of
the requirements for the degree of Doctor
of Philosophy in the University Program in
Genetics and Genomics in the Graduate School
of Duke University

2013

ABSTRACT

Mechanisms Underlying Bone Cell Recovery During Zebrafish Fin Regeneration

by

Sumeet Pal Singh

University Program in Genetics and Genomics
Duke University

Date:_____
Approved:

_____
Kenneth Poss, Supervisor

_____
Blanche Capel, Chair

_____
Scott Soderling

_____
Michel Bagnat

An abstract of a dissertation submitted in partial
fulfillment of the requirements for the degree
of Doctor of Philosophy in the University Program in
Genetics and Genomics in the Graduate School of
Duke University

2013

Abstract

Zebrafish regenerate amputated caudal fins, restoring the size and shape of the original appendage. Regeneration requires generation of diverse cell types comprising the adult fin tissue. Knowledge of the cellular source of new cells and the molecules involved is fundamental to our understanding of regenerative responses. In this dissertation, the contribution made by the bone cells towards fin regeneration is investigated. Fate mapping of osteoblasts revealed that spared osteoblasts contribute only to regenerating osteoblasts and not to other cell types, thereby suggesting lineage restriction during fin regeneration. The functional significance of osteoblast contribution to fin regeneration is tested by developing an osteoblast ablation tool capable of drug induced loss of bone cells. Normal fin regeneration in the absence of resident osteoblast population suggests that the osteoblast contribution is dispensable and provides evidence for cellular plasticity during fin regeneration. To uncover the genes involved in proliferation of osteoblasts within the fin regenerate, a candidate in-situ screen was carried out and revealed bone specific expression of *fgfr4* and *twist3*. Transgenic tools for visualization of gene expression confirmed the screen results. Knockdown of *twist3* by morpholino antisense technology impedes fin regeneration. Mutant heterozygotes for *twist3* were generated using genome editing reagents, which will enable loss-of-function study in future.

Contents

List of Figures

1. Introduction

1.1 Key Questions in Regenerative Studies

Ancient myths and folklore suggest that humans have been aware of regeneration for a long time. The remarkable story of Prometheus in Greek mythology is an elegant example of fantastical regeneration. Prometheus was punished by Gods for bringing fire to humans, which symbolized knowledge. He was bound by chains in faraway mountains and an eagle would come and eat his liver every day. However, every night his liver would regenerate and Prometheus would continue to live through endless suffering. Although the rapidity of liver regeneration suggested is superhuman, the story indicates ancient fascination with growing back lost parts of the body.

The potential significance to human wellbeing made regeneration one of the oldest fields in biology (Dinsmore, 1991). Regenerative phenomena were described in writings of Aristotle, and the first scientific observations were reported in 1712 by René-Antoine Ferchault de Réaumur, who made a detailed description of limb regeneration in crayfish. The next half century saw seminal investigations on regeneration in hydra by Abraham Trembley in 1740, amphibians by Spallanzani (1769), among other organisms. Description of regeneration in multiple animals continued but was confined to gross observations. At the end of nineteenth century Thomas Hunt Morgan (1901) lead an active school of regeneration research using fish and planarians. Morgan labeled the gut of planarians with red color by feeding them the strongly pigmented eyes of adult

Drosophila; which he chose as his model organism for study of genetics after becoming overwhelmed with the complexity of regeneration, ultimately to the benefit of biology.

Over such a long period of time, three questions developed to be the center of regeneration biology:

1. Why do some organisms regenerate while other don't.
2. Which cells respond to injury and fill the missing part.
3. What genes are involved in injury response and how similar are they to the ones involved during embryonic development.

The first question or the evolutionary aspect of regeneration provides the motivation behind regenerative studies. Virtually all species, from protozoa to humans, have the capacity to regenerate, but the extent of their regenerative ability varies greatly. Planarian, starfish and some worms can regenerate most of their body, whereas many other species are able to regenerate only parts of specific tissues. Among vertebrates, urodele amphibians and certain fish are best adapted for regeneration; they can regenerate limbs, jaws, eyes, and a variety of internal structures. Understanding examples of successful regeneration will, hopefully, empower us to stimulate it in humans.

Stimulation of regeneration in regeneration-deficient species requires knowledge of the last two questions. For example, studies in certain planarians has established stem cells (neoblast) to be the cellular source of regeneration, and Wnt signaling to regulate

their ability to regenerate head structures. This information was used to rescue lack of head regeneration in multiple related planarian species (Liu et al., 2013; Sikes and Newmark, 2013; Umesono et al., 2013).

Insights from various models of regeneration will similarly help realize the dream of regenerating human organs.

1.2 Appendage Regeneration

Humans have limited limb regeneration capacity. Age is a substantial determinant of the limitations of mammalian appendage regeneration (McKim, 1932; Vidal and Dickson, 1993). Spontaneous human fingertip regeneration has been reported in children, but rarely in adults. In successful cases, only the distal fingertip past the joint can recover from amputation, even if the loss includes proximal regions: A 4-year-old female sustained an amputation of the 4th digit at the proximal interphalangeal joint with loss of both the middle and distal finger segments. She received no surgical interventions and the finger was allowed to heal naturally. When seen 18 years later, she had a fully formed distal segment (with a vestigial nail) that articulated directly with the proximal segment. X-ray showed that the 4th digit had developed a distal phalanx (Cobiella et al., 1997). This was not simply a case of healing. The fact that an entire distal phalanx grew at the level of the proximal interphalangeal joint without the presence of a middle segment is a clear expression of the ability to regenerate fingertips only.

Newborn and adult mice too can regenerate amputated digit tips within a few months. In contrast, certain amphibians and fish species are capable of whole-limb regeneration. Upon amputation, a remarkable series of regenerative stages are initiated that result in the complete restoration of lost tissue. This complex process, termed epimorphic regeneration, involves the formation of a mass of undifferentiated proliferative cells called a blastema (Akimenko et al., 2003; Gemberling et al., 2013; Poss, 2010; Poss et al., 2003; Yin and Poss, 2008). Immediately following surgical removal of limb tissue an initial wound healing stage, characterized by nonproliferative lateral epithelial cell migration over the wound and subsequent formation of the apical epidermal cap (AEC), is initiated (Nechiporuk and Keating, 2002). Second, the wound epithelium thickens and mesenchymal tissue proximal to the amputation plane begins to disorganize. Cellular disorganization is thought to occur as a result of growth factors that originate from the mature wound epidermis and stimulate mesenchymal cells to dedifferentiate and proliferate as they migrate distally towards the area directly proximal to the AEC. In the third stage, the blastema forms at the distal mesenchyme compartment. Blastema formation is the main event that distinguishes regeneration from limb development. The blastema is an accumulated mass of progenitor cells that are able to produce daughter cells capable of differentiating into a variety of cell types required to populate the regenerating tissue.

The next phase of regenerative outgrowth is marked by intense proliferation in the blastema. A moderately proliferative patterning zone is located immediately proximal to the blastema. The patterning zone contains newly divided cells that migrate to appropriate locations and differentiate to populate the new tissue. The location and functional differences within the blastema and patterning zone are thought to be generated and maintained through epithelial-mesenchymal interactions (Lee et al., 2009). The final stage, regenerative termination, is not well understood. Fin regeneration proceeds rapidly until the preamputation fin length is reached, at which point it switches to an ontogenetic growth mechanism. It is speculated that termination occurs by either an unknown active termination mechanism or by cessation of regenerative signaling (Iovine, 2007).

1.3 Differentiation Potency of Blastema Cells

Over the last century, researchers have debated how far backward limb cells reverse their commitment during blastema formation. During early development, pluripotent cells first commit to a germ layer (ectoderm, mesoderm, or endoderm), and then each germ layer diversifies into differently committed progenitors that establish the various tissue subtypes. The limb is built primarily from several subtypes of mesoderm, including lateral plate mesoderm that forms dermis, connective fibroblasts, and skeletal elements as well as somitic mesoderm that forms limb muscle. Blood vessels may arise from lateral plate or somitic mesoderm. The ectoderm forms the limb epidermis,

whereas the neural crest, which derives from neurectoderm, contributes Schwann cells and melanocytes.

Prior to molecular genetic labeling, it was difficult to conclusively resolve whether cells reverted to a fully pluripotent state or to a more restricted progenitor cell type during blastema cell formation. Grafting experiments in amphibians performed over the past century have attempted to resolve this issue. Blastemas were grafted onto ectopic sites, or nonirradiated limb tissue was grafted onto irradiated limb hosts to evaluate differentiation potential (Namenwirth, 1974). Alternatively, grafting of tritiated thymidine-labeled or triploid limb tissues was used to assess which tissue contributed cells to the blastema and their potency (Steen, 1968). Surgical transplantation of dissected cartilage or bone indicated that skeletal tissues wholly or predominantly contribute like tissue, suggesting that lineage is restricted throughout blastema formation and patterning (Namenwirth, 1974; Steen, 1968; Steen, 1970). Yet, other experiments, including the transplantation of dye-labeled muscle cells to limb blastemas or non-skeletal tissue to irradiated limbs, indicated that additional cell types may act as progenitors for bone or cartilage (Lo et al., 1993; Morrison et al., 2006). Major drawback of such studies was the use of cell shape and cytoplasmic features instead of molecular markers to identify cell types.

The blastema cell potency issue was revisited in amphibians using cells harboring a genomically inserted green fluorescent protein (GFP) transgene. The results

indicated that blastema cells deriving from the different limb tissues remain restricted to lineages related to their embryonic origin (Kragl et al., 2009). For example, dermis cells could form cartilage (both of which derive from lateral plate mesoderm), but not muscle, which derives from somites, and vice versa. Schwann cells, which are of neural crest origin, did not form muscle or cartilage. In this work, instead of using limb tissue grafting, which labels a complex mixture of different cell types including blood vessels, peripheral nerves, and connective tissue, GFP^{+} precursor populations for a given limb tissue were transplanted at embryonic stages. Therefore, it was possible to screen for animals with accurate tissue labeling via GFP signal prior to starting the experiment and therefore obtain consistent, interpretable results.

1.4 Source of Bone Cells During Fin Regeneration

Zebrafish caudal fins are complex structures that contain 16–18 lepidotrichia (fin rays) connected by soft tissue interrays that lack skeletal elements. The fin rays are a series of bony segments comprised of a pair of concave hemirays surrounded by a monolayer of osteoblasts (bone-secreting cells). The hemirays function to protect an intraray core consisting of blood vessels, nerves, melanocytes and fibroblasts. Fibroblasts are also present in the interray space. The entire multi-ray fin is covered by an epithelial cell layer. The fin displays an indeterminate ontogenetic growth pattern, meaning that fin growth occurs by the gradual addition of bony ray segments to the distal tip of the fin.

Upon amputation, fin recovers by epimorphic regeneration. Epithelium covers the injured fin within 24 hrs and blastema formation occurs from 24-48 hrs. The cells in blastema proliferates slowly with a median G2 cell cycle time of >6 h (Nechiporuk and Keating, 2002). Twenty-four hours following caudal fin amputation, blastemal cells segregate into two morphologically identical, but functionally distinct, subpopulations. The distal blastema, located proximally to the AEC, proliferates extremely slowly. In sharp contrast, the proximal blastema proliferates rapidly with a mean G2 time of <60 min. Together, the proximal and distal blastema form a proliferation gradient with a 50-fold difference in proliferation across an approximate distance of 50 μM or 10 cell diameters (Nechiporuk and Keating, 2002).

A major objective in the field has been to define the cellular source(s) of regenerated skeletal elements. This includes identifying cell types within the appendage stump that normally give rise to regenerated cartilage or bone after amputation, as well as identifying cells that have the developmental capacity to create skeleton under additional conditions (Poss, 2010; Tanaka and Reddien, 2011). Proposed sources are the differentiated chondrocytes and osteoblasts themselves, or non-skeletal cells that undergo new differentiation or trans-differentiation events after amputation. The recent study of axolotl limb regeneration generated the prevailing model for limb regeneration, in which is the cartilage cells predominantly contribute to like tissue, while one or more

cell populations within the dermis also has the potential to form cartilage (Kragl et al., 2009).

Certain key questions of tissue origin remain unresolved, such as: 1) how host tissue naturally participates in regeneration; 2) the extent to which specific cell types contribute during regeneration; and 3) whether cells in the stump undergo developmental changes like de-differentiation in the process of creating new structures. Multiple studies have examined similar questions during fin regeneration in zebrafish by genetic lineage-tracing of specific cell types. By inducible fate-mapping of cells expressing the intermediate osteoblast marker *osterix*, Knopf and colleagues found that existing osteoblasts undergo partial de-differentiation, as defined by reduced expression of osteoblast markers, after which they proliferate and contribute solely to regenerated bone structures (Knopf et al., 2011). Tu and Stewart with their respective colleagues assessed the mosaicism of transgenes induced into embryos during rapid cell division, and found that transgenic clones containing labeled osteoblasts within regenerated fins do not possess other cell types (Tu and Johnson, 2011; Stewart and Stankunas, 2012). Sousa and colleagues used live imaging of labeled *osteocalcin*-expressing cells to indicate contribution of differentiated osteoblasts to the regenerate (Sousa et al., 2011). Together, these studies supported a common conception that osteoblasts in the regenerate derive predominantly or wholly from the de-differentiation, proliferation, and migration of lineage-restricted stump osteoblasts.

By creating a system to facilitate inducible ablation of resident osteoblasts in adult fins, this dissertation examines the extent to which zebrafish fin regeneration is dependent on these cells. Lineage-tracing of existing osteoblasts found that they are restricted to contributing like cells during regeneration, in agreement with previous work. Unexpectedly however, ablation of ostensibly all osteoblasts prior to amputation did not slow down the rate of zebrafish fin regeneration. Instead, new osteoblasts arose from cells that differentiated de novo after amputation, a result confirmed by genetic fate-mapping. The findings indicate that stump osteoblasts are a dispensable source for regenerating appendage bone, and provide important new context for understanding mechanisms of robust skeletal regeneration.

2. Material and Methods

2.1 Zebrafish Husbandry and Strains

Wild-type or transgenic zebrafish of the outbred Ekkwill (EK) or a hybrid EK/AB strain of 4-6 months of age were used for all experiments. Caudal fin amputations were performed with a razor blade on fish anesthetized with tricaine, and removed one-half of fins. The transgenic *β-act2:RSG* line has been described previously (Kikuchi et al., 2010). *osx:mCherry*, *osx:Kaede* and *osc:EGFP* constructs were generated by subcloning *mCherry*, *Kaede* and *EGFP* cassettes respectively downstream of published promoter sequences of medaka *osterix* or *osteocalcin* genes (Inohaya et al., 2007; Renn and Winkler, 2009). For *osx:NTR*, we subcloned *mCherry*, fused to a human codon-optimized version of the *Escherichia coli* enzyme Nitroreductase, downstream of the *osterix* regulatory fragment (Grohmann et al., 2009). To generate *osx:CreER*, a bicistronic construct containing the coding sequence for *mTagBFP* (Evrogen) (Subach et al., 2008) and sequences encoding a tamoxifen-inducible Cre recombinase-estrogen receptor fusion protein, separated by a 2A viral linker sequence (Trichas et al., 2008), were subcloned downstream of the *osterix* promoter. *mTagBFP* aided visualization of *CreER* expression in embryos, useful for identifying and maintaining the transgenic line. Plasmid constructs

were co-injected with I-SceI into one-cell zebrafish embryos for linearization, and all transgenic strains were analyzed as hemizygotes.

To generate BAC transgenic animals *fgfr4:EGFP* and *ColX:mCherry* the translational start codon of *fgfr4*and *ColX* in the BAC clone CH211-281E1 and CH211-266G18 was replaced with the *EGFP* and *mCherry* cassette respectively by Red/ET recombineering technology (GeneBridges). The 5′ and 3′ homologous arms for recombination were a 50-base-pair (bp) fragment upstream of the start codon, and a 50-bp fragment downstream, respectively, and were included in PCR primers to flank the *EGFP* and *mCherry* cassette. The final BAC was purified with Nucleobond BAC 100 kit (Clontech), and co-injected with PI-*Sce*I into one-cell-stage zebrafish embryos.

For 4-HT labeling, adult zebrafish were incubated with aquarium water containing 5 μM 4-HT, made from a 1 mM stock solution in 100% ethanol. Fish were maintained in 4-HT in the dark for the indicated periods of time, and then were rinsed and returned to recirculating aquarium water. For osteoblast ablation, fish were incubated with 10 mM Mtz (Sigma, M1547) dissolved in aquarium water, and maintained for 24 hours in the dark before they were rinsed and returned to recirculating aquarium water.

Photoconversion of *osx:Kaede* was carried out by exposing caudal fin to ultraviolet light by means of DAPI filter of compound microscope. Anesthetized zebrafish were gently laid on glass slide, which was then inserted in a compound

microscope. The caudal fin was brought into focus using the green channel. Exposure to ultraviolet light was carried out for 2 min. Successful photoconversion was verified by lack of signal in green channel.

2.2 Fin Length Measurement and Analysis

Leica Application Suite software was used to measure fin regenerates from images of live, anaesthetized fish. The distances from the amputation plane to the distal tips of the 2nd and 3rd lateral-most rays on the dorsal lobe was measured. These lengths were averaged to give one value per animal. Unpaired Student's t-tests were performed to determine p-values.

2.3 Histological Methods

TUNEL staining on whole-mount fins was performed using a previously described protocol (Wills et al., 2008). For BrdU-labeling experiments, animals were injected intraperitoneally with ~0.05 ml of a 2.5 mg/ml solution of BrdU dissolved in water. BrdU was injected 5 hours before fin collection, and immunodetection of BrdU was performed as described (Lee et al., 2005). In situ hybridization on cryosections was performed using digoxygenin-labeled RNA probes as described previously (Poss et al., 2002). The monoclonal Zns5 (1:50 dilution; Zebrafish International Resource Center), polyclonal DsRed (1:500 dilution; Clontech) and polyclonal p63 (1:200 dilution; Abcam) antibodies were used for immunofluorescence analysis.

2.4 Flow Cytometry

Adult zebrafish caudal fins were amputated and dissociated by vigorous shaking for 20 minutes at room temperature in a solution of Liberase DH Research Grade (Roche) reconstituted in Hank's Buffered Salt Solution (HBSS) buffer. The cells were briefly spun down and resuspended in HBSS, and then passed through a 40-μm filter. Propidium iodide (Sigma) was added to a concentratin of 1 μg/ml. Flow cytometry analysis was performed using a BD FACSCanto II (BD Biosciences), using forward and side scatter parameters to exclude cell debris.

2.5 twist3 TALEN design

The software developed by the Bogdanove laboratory (https://boglab.plp.iastate.edu/node/add/talen) was initially used to find candidate binding sites (Cermak et al., 2011a). Three criteria were used for TALEN design. First, TALEN binding sites were selected in area with least conservation among *twist3* sequences found in NCBI (Figure 18). Second, TALEN cut sequences were selected around a restriction enzyme centrally located within the spacer for ease of screening. Third, HA-epitope tag insertion fusion at the site of double strand break was synthesized in-vitro and tested for its nuclear localizing activity (Figure 19).

Using these two criteria, the *twist3* TALEN recognition sequences were: left TALEN 5′-TTGTGGAGATTTTCCT-3′ and right TALEN 5′-TGCTCTTCTTCAATGGG-

3′. Between the two binding sites is a 15-bp spacer with *BamHI* site (GAAAGTGGGATCCTT, *BamHI* underlined)

2.6 TALEN Construction

TALEN assembly of the RVD-containing repeats was conducted using the Golden Gate approach (Cermak et al., 2011b). Once assembled, the RVDs were cloned into a pCS2TAL3 destination vector with the appropriate backbone (DD for left, RR for right) to generate mRNA expression plasmids (Dahlem et al., 2012). *In vitro* transcription of TALEN mRNA was conducted by linearizing the expression plasmids with *NotI* endonuclease at 37 °C for 2–3 h, transcribing the linearized DNA (SP6 mMessage Machine kit, Ambion) and purifying the mRNA by phenol/chloroform extraction (SP6 mMessage Machine kit user manual protocol) for injection.

2.7 TALEN Mutation Screening

One-cell embryos were microinjected with 25 pg of TALEN mRNA. Genomic DNA for testing TALEN activity was collected at 2 days post-fertilization from individual larvae. Genomic DNA for screening *twist3* mutants was isolated from groups of 10 larval zebrafish. Genotyping was conducted using PCR followed by restriction enzyme digest. For *twist3*, the primers were 5′-ACCCAAAGCAATGGCTGTAT-3′ and 5′-GGATCAGAGTTCGGGATTCA-3′. Mutations were assessed by loss of restriction enzyme digestion. To sequence-verify mutations, the gel-purified, uncut PCR products were cloned into the pJet1.2 Cloning Kit (Thermo Scientific).

2.8 Genome Editing

For the *twist3* locus, a ssDNA oligonucleotide was designed to target the spacer sequence between the TALEN cut sites. The oligonucleotide extends across the length of the TALEN recognition site. An HA-epitope tag (5′-TACCCATATGATGTTCCAGATTACGCT-3′) was introduced at the site of double strand break resulting in a 59-base homology arm on the 5′ end and a 51-base homology arm on the 3′ end. The complete sequence of oligonucleotide is 5′-GGACTGATCGTCATGCGAGAGGAACAGACTTGTGGAGATTTTCCTGAAAGTGGGATCTACCCATATGATGTTCCAGATTACGCTCTTCCCATTGAAGAAGAGCAGGAGCGGCGCCCCAATAAGTGTGCGGTTG-3′. The oligonucleotide was ordered from Integrated DNA Technologies (IDT).

One-cell embryos were microinjected with both the GoldyTALEN mRNA and ssDNA donor (25 pg each). Genomic DNA was isolated and PCR was conducted using HA-tag specific FP (5′-CCCATATGATGTTCCAGATTACG-3′) and *twist3* screening RP (above). Injected fish from the same batch of somatically screened embryos were raised. When the fish were at least two months old, fin tissue was obtained for finding germline founder. The fish were anesthetized using Tricaine (approximately 200 $\mu g\ ml^{-1}$). The tail fins were trimmed with a fresh razor blade for each fish to prevent contamination. The most caudal 2–3 mm of fin was biopsied and placed on ice until all fin biopsies were collected. Genomic DNA was isolated and PCR performed with HA-primer and *twist3*

screening RP (above). Those fish that maintained somatic modifications were outcrossed to wild-type fish and the embryos were screened for germline modification. Genomic DNA with germline events was again PCR amplified using *twist3* screening FP and RP, cloned and sequenced to verify precise insertion.

2.9 Morpholino Based Knockdown of twist3

Vivo-porter coupled morpholino oligonucleotide (MO) (Gene Tools) was used at 0.25 mM for injection. The morpholino was designed complementary to *twist3* translation-initiation site. The MO sequence was (5′ to 3′):

CACAAGTCTGTTCCTCTCGCATGAC.

MO was injected in the dorsal half of the fin regenerate at 48 hpa (Demonstration of the injection procedure can be found here (Hyde et al., 2012)). The other uninjected half was considered as the internal control in order to monitor the normal growth. Immediately after injection the fins were photographed using a stereomicroscope. The same fins were again photographed at 24 hours after morpholino delivery.

The software ImageJ 1.42h was used for the measurement of the regenerate area. In order to calculate the percentage area of the outgrowth between the injected and non-injected part, the values were inserted in the following formula: $(Exp_{3\ days} - Exp_{2\ days})/(Cont_{3\ days} - Cont_{2\ days}) \times 100$, where Exp is the area of the outgrowth of the MO-treated regenerate and Cont is the area of the corresponding outgrowth of the uninjected control half.

3. Results

3.1 Plasticity in Bone Cell Source During Zebrafish Fin Regeneration

(Sections adapted from Singh S.P., Holdway J.E. and Poss K. D. 2012. Regeneration of Amputated Zebrafish Fin Rays from De Novo. *Dev. Cell.* 22, 879–886)

3.1.1 Promoters Driving Osteoblast Specific Expression

Several candidate genes were screened for bone-specific expression as a prerequisite for genetic fate-mapping. *osterix* (also known as *sp7*) is a zinc finger transcription factor whose expression is first seen during intermediate stages of osteoblast differentiation (Li et al., 2009; Renn and Winkler, 2009). *osteocalcin* (also known as *bglap*), expressed by mature osteoblasts, has been used as a marker of terminal osteogenesis (Inohaya et al., 2007). Transgenic reporter lines were generated to visualize the activity of the teleost *osterix* and *osteocalcin* regulatory sequences. Tg(*osterix:mCherry*) (*osx:mCherry*) and Tg(*osteocalcin:EGFP*) (*osc:EGFP*) each showed osteoblast-specific fluorescence in uninjured adult zebrafish fins that was excluded from medially located fibroblasts and from epidermis. *osx:mCherry* visualized a larger pool of osteoblasts than *osc:EGFP* (Figure 1A-D). Regenerated osteoblasts labeled by *osterix*-driven *mCherry* expression could be detected as early as 2 days post-amputation (dpa), while *osteocalcin*-

driven *EGFP* expression was not detectable until 7 dpa (Figure 1E-H).

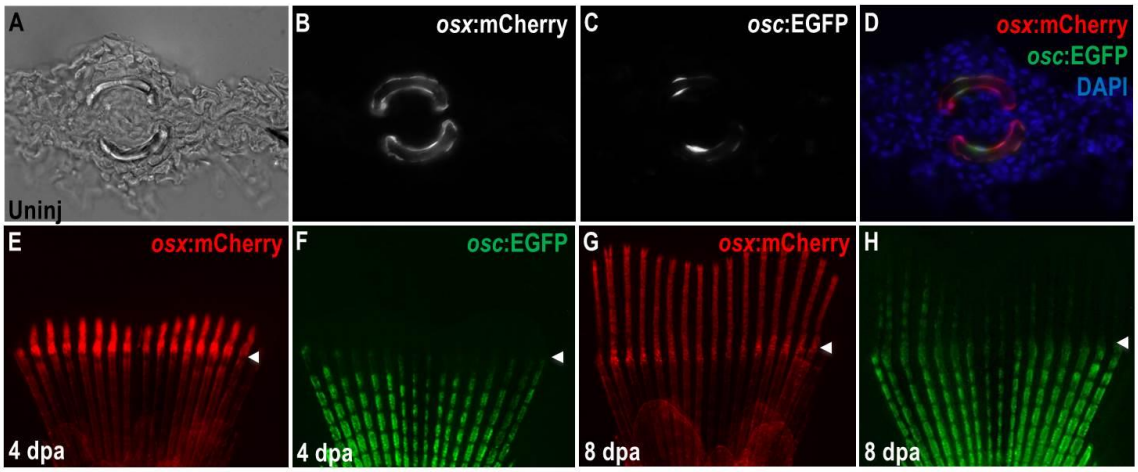

Figure 1: Osteoblast-Specific Transgenic Reporter

(A-D) Transverse section through an uninjured caudal fin from an *osx:mCherry; osc:EGFP* double transgenic animal. Fin hemirays are outlined by *osx:*mCherry^{+} osteoblasts, most of which are also positive for *osc:*EGFP fluorescence. **(E-H)** Regenerating fins of *osx:mCherry; osc:EGFP* animals shown at 4 (E, F) and 8 (G, H) dpa. *osx:*mCherry is easily visible in the regenerate by 4 dpa, while *osc:*EGFP fluorescence emerges at 7-8 dpa. Arrowheads indicate amputation planes.

3.1.2 Osteoblast Contribution is Lineage Restricted

Genetic fate mapping approaches were undertaken to identify contributions by differentiated osteoblasts towards fin regenerate. For Cre/Lox based lineage tracing, a transgenic line was generated with *osterix* regulatory sequences driving a tamoxifen-inducible Cre recombinase-Estrogen receptor fusion protein Tg(*osterix:mTagBFP-2A-CreER*) (*osx:CreER*) (Figure 2A). An indicator line, Tg(*bactin2-Lox-DsRed-STOP-Lox-*

EGFP) (*β-act2:RSG*) permitted visualization of *EGFP* fluorescence after Cre-mediated excision of loxP-flanked stop sequences, and was expressed in adult osteoblasts, intraray fibroblasts, and epidermis (Figure 2B) (Kikuchi et al., 2010).

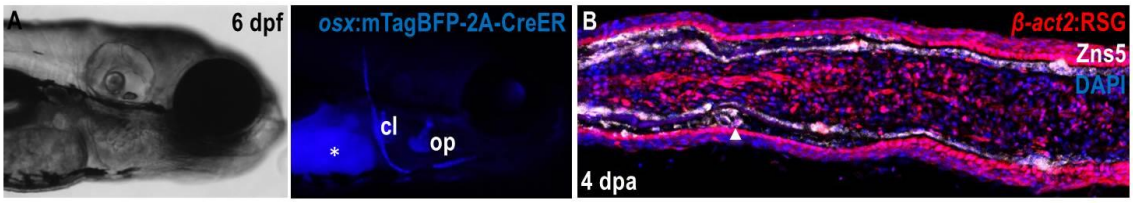

Figure 2: Lineage-Tracing Strains

(A) Bright field (left) and fluorescent (right) images of a 6 dpf *osx:CreER* larva, indicating blue mTagBFP fluorescence in bone structures. Asterisk, yolk autofluorescence. cl, clethium; op, opercule. **(B)** Section through a 4 dpa *β-act2:RSG* fin regenerate. DsRed fluorescence is detectable in most cells, indicating that the line is suitable for genetic fate-mapping of fin tissues.

To label osteoblasts, *osx:CreER*; *β-act2:RSG* animals were incubated with 4-hydroxytamoxifen (4-HT) or vehicle for one day (Figure 3A). Within 2 days, EGFP+ cells were visible lining the osteoblast compartment of fin rays treated with 4-HT only (Figure 3B-3E). No EGFP+ cells were observed in intraray fibroblasts, located medially to osteoblasts in longitudinal fin sections. These data indicate that *osx:CreER* inducibly and specifically labels osteoblasts.

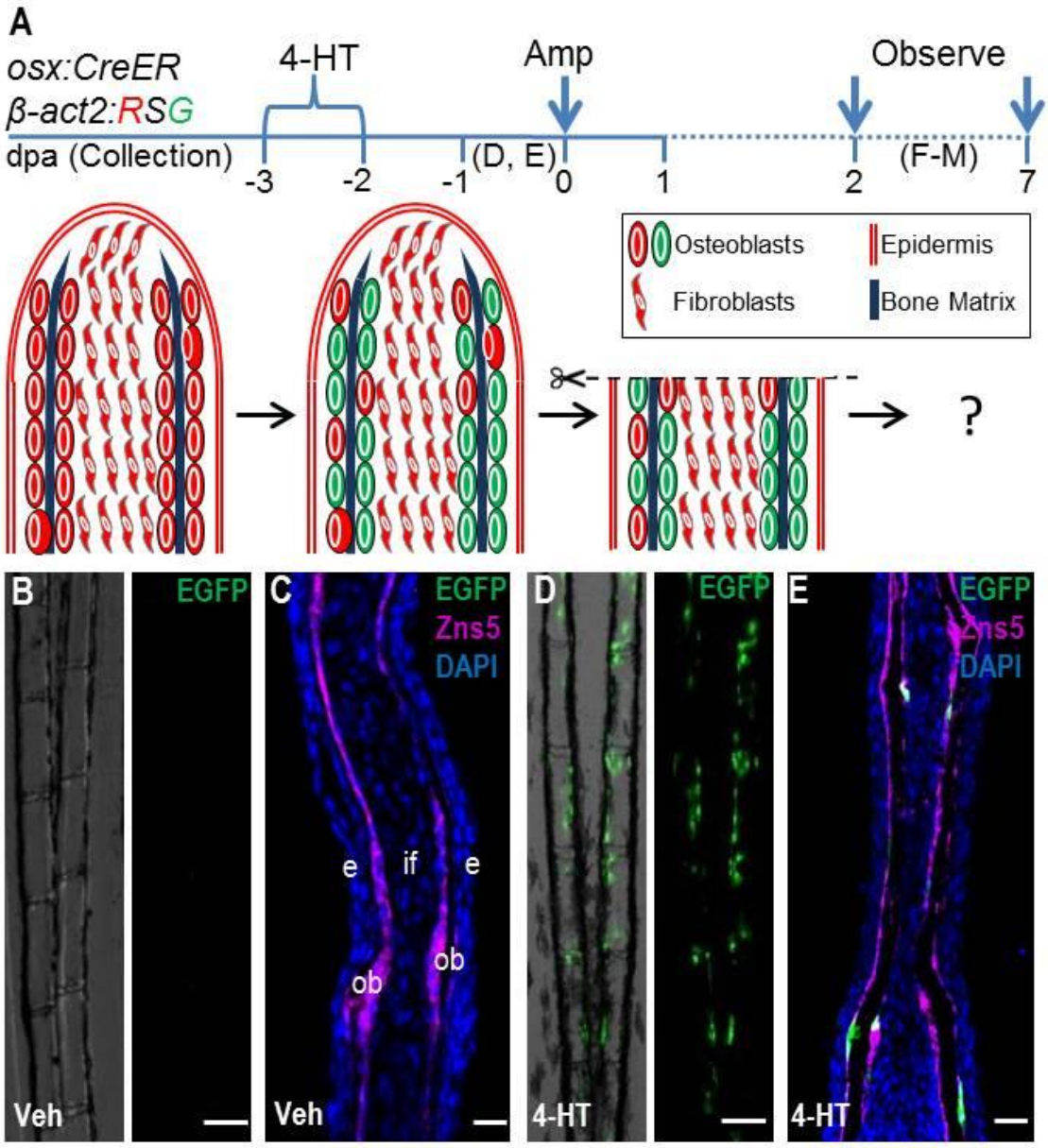

Figure 3: Lineage Tracing Resident Osteoblasts

(A) Cartoon summarizing strategy for inducible, genetic fate-mapping of osteoblasts during zebrafish fin regeneration. 4-HT treatment labels *osterix*-expressing cells with EGFP prior to amputation. **(B, C)** Uninjured *osx:CreER; β-act2:RSG* fins, shown as whole

mount (B) and in a longitudinal section (C), display no labeling after vehicle treatment. Zns5 (magenta) is an uncharacterized antigen that helps identify osteoblasts lining hemiray bone. This antibody stains cell membranes and visualizes as non-contiguous staining in sections. (C) The longitudinal fin section is labeled to show structures: intraray fibroblasts (if), osteoblasts (ob), and epidermis (e). **(D, E)** 4-HT treatment labels many osteoblasts with EGFP in uninjured fins, shown as a whole-mount image (D) and a longitudinal section (E). Scale bars = 100 μm.

To examine the contribution of *osx*-expressing cells to the regenerate, the caudal fins of zebrafish were amputated at 2 days after 4-HT treatment (Figure 3A). EGFP+ cells were detected in regenerating fins from 2 dpa onwards, a result that indicated contribution from osteoblasts within the stump. As regeneration progressed to 3, 4 and 7 dpa, the domain of EGFP+ expression expanded distally within the regenerate. Confocal analysis of fin sections at 2, 3, 4, and 7 dpa revealed EGFP+ cells confined to regions lining bone matrix both below and above the amputation plane, indicating that a population of osteoblasts in the regenerate is derived from stump osteoblasts. No EGFP+ expression was observed in intraray fibroblasts or other cell types (Figure 4).

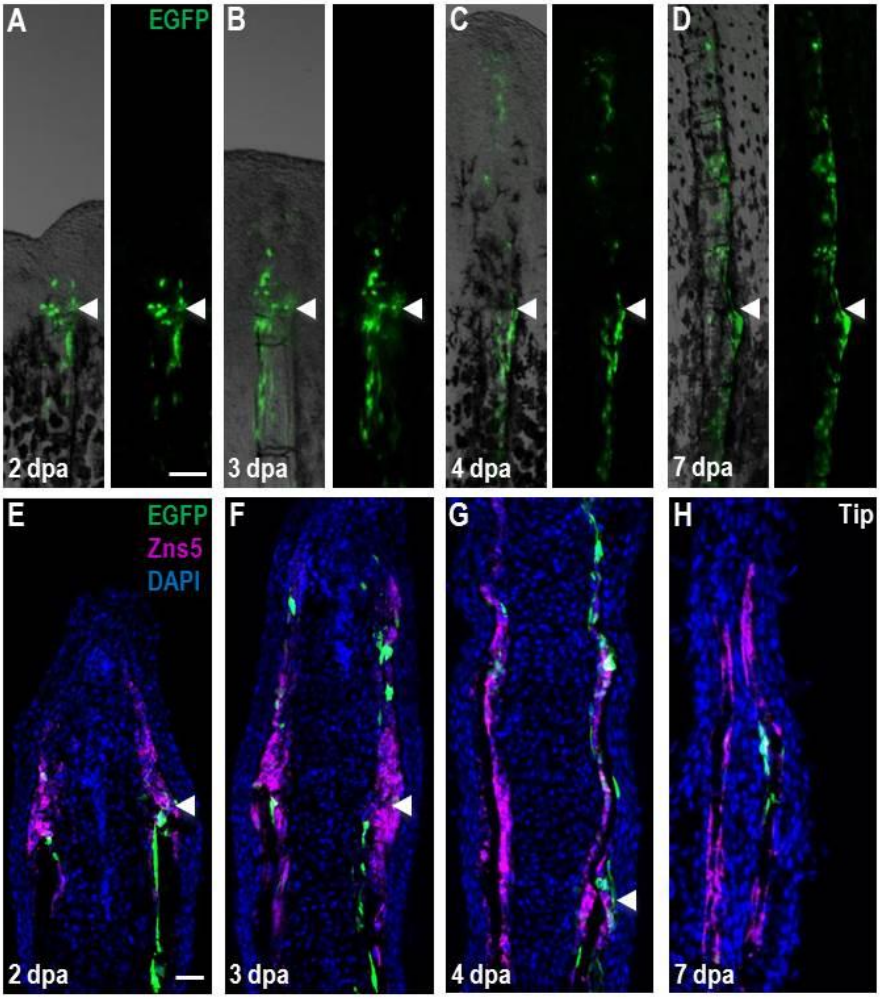

Figure 4: Resident Osteoblasts Contribute New Osteoblasts to Regenerating Fin Structures

(A-H) EGFP^{+} osteoblasts labeled by 4-HT treatment prior to fin amputation contribute labeled progeny to the regenerate, visualized by whole-mount images and in sections at 2 (A, E), 3 (B, F), 4 (C, G), and 7 (D, H) dpa. EGFP fluorescence proximal and distal to the amputation plane is restricted to the osteoblast compartment and is not present in intraray fibroblasts or epidermis. Arrowheads indicate the plane of amputation. Scale bars = 100 μm.

The efficiency of *CreER* based recombination in zebrafish fin is significantly less than 100%. This prevents us from accessing the contribution from other potential sources, if any. We took advantage of photoconvertable *Kaede* to comprehensively label the osteoblast population. Transgenic line driving *Kaede* from *osx* regulatory sequence (*osx:Kaede*) were established. Without exposure to ultraviolet light, the fins emitted green fluorescence with little to no red red fluorescence (Figure 5A). Upon ultraviolet light exposure for 2 min, all green fluorescence in caudal fin changes irreversibly to red, thereby labeling the spared osteoblasts with red color (Figure 5B). The cells can be followed until the red fluorescence is lost in cells due to protein turnover or dilution by cell cycle.

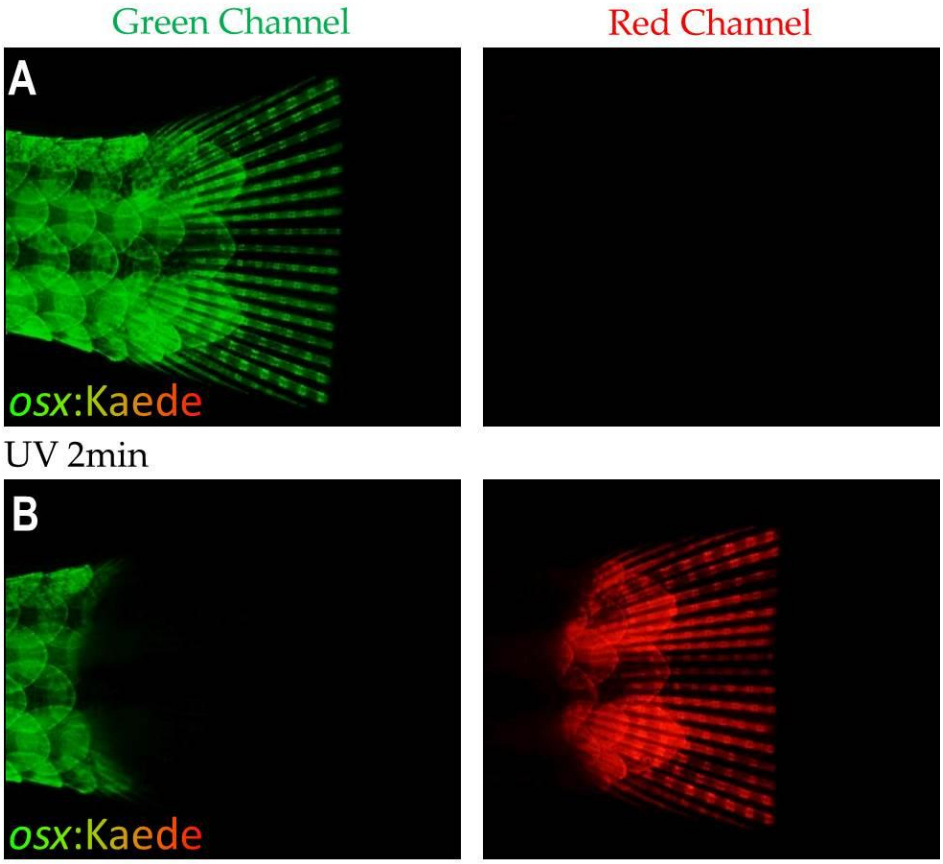

Figure 5: Photoconversion of *osx:Kaede* Fins

(A) osx:Kaede transgenic fin without exposure to UV light shows bright fluorescence in green channel and none in red channel. **(B)** After 2 min exposure to UV light, the green fluorescence inside the exposed area changes to red.

Analysis of fin tissue subsequent to *Kaede* labeling and amputation reveals that all new osteoblast cells in the regenerate, marked by green fluorescence, are derived from spared osteoblasts, labeled with red fluorescence (Figure 6). This shows absence of any contribution from other cell types towards regenerating osteoblast population.

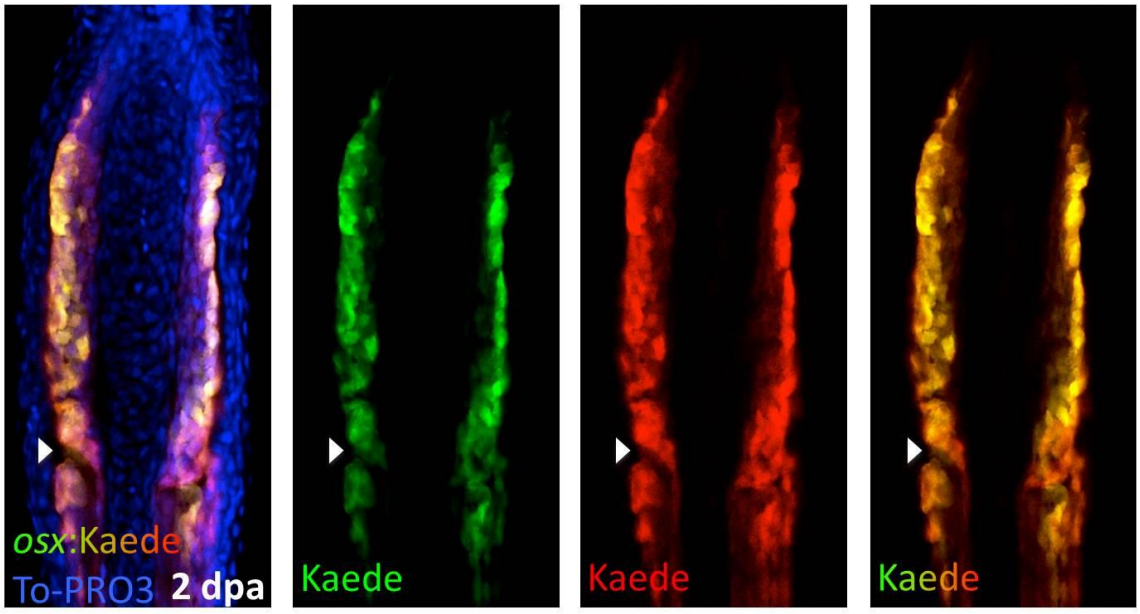

Figure 6: Spared Osteoblasts are the Only Source of Regenerating Osteoblasts

A 2 dpa transverse sections across photoconverted *osx:Kaede* shows all cells contributing the regenerating osteoblast population (green) also harbor red Kaede fluorescence, thereby suggesting that they are derived from osteoblasts spared from fin amputation.

The two lineage tracing experiments taken together suggest the lack of contribution from osteoblasts lineage to other ones and vice versa in the regenerating zebrafish fin.

3.1.3 Genetic Ablation of Zebrafish Osteoblasts

Although these data indicated that spared osteoblasts contribute new bone during regeneration, we and others (Knopf et al., 2011; Sousa et al., 2011) could not address the extent to which fin regeneration is dependent on cellular contributions by resident osteoblasts. To probe the regenerative capacity of zebrafish fins after massive osteoblast loss, we generated a transgenic line containing a *mCherry*-tagged, human codon-optimized version of the *Escherichia coli* enzyme Nitroreductase (NTR) downstream of *osterix* regulatory sequences, Tg(*osterix:mCherry-NTRo*) (*osx:NTR*) (Grohmann et al., 2009). NTR reduces exogenously added metronidazole (Mtz) pro-drug to form a cytotoxic product with negligible bystander effects, and has been employed successfully to ablate specific cell types in zebrafish larvae (Curado et al., 2007). Treatment of *osx:NTR; osc:EGFP* fish for 24 hours with 10mM Mtz caused a dramatic loss of *osx*- and *osc*-driven fluorescence throughout the fish by 4 days post-treatment (dpt) (Figure 7A). We did not observe impaired movement or behavior in these animals. TUNEL staining of caudal fins indicated extensive induction of apoptosis in osteoblasts lining the fin bone of *osx:NTR* fish that had been treated one day prior with Mtz (Figure 7B, C).

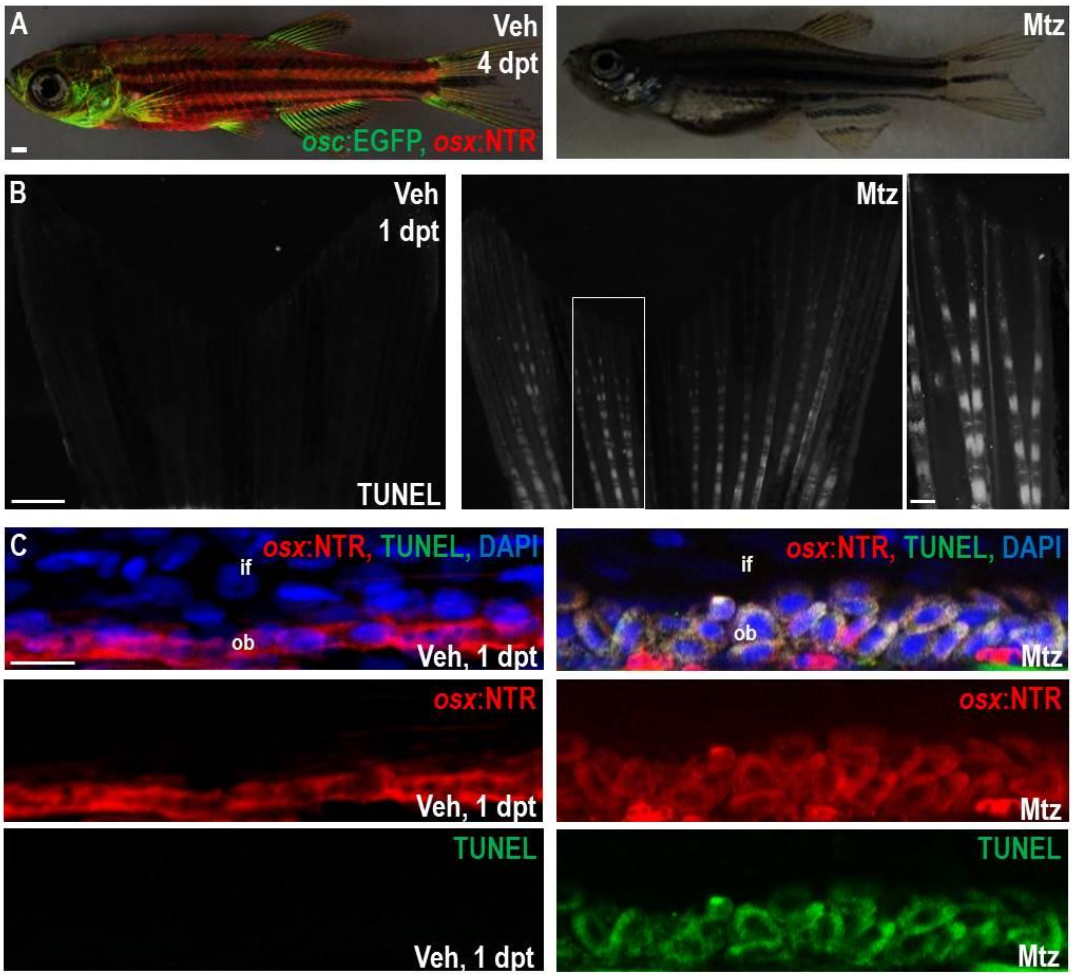

Figure 7: Inducible Ablation of Adult Zebrafish Osteoblasts

(A) Juvenile *osx:NTR; osc:EGFP* fish treated with vehicle (left) or Mtz (right) and assessed for fluorescence 4 days later. There was no detectable marker expression in Mtz-treated animals. Scale bar = 1 mm. **(B, C)** TUNEL staining of *osx:NTR* fins 24 hours after vehicle (left) or Mtz (right) treatment, indicating profound, osteoblast-specific apoptosis in Mtz-treated fish. Higher magnification images the atypical rounded appearance 24 hours after Mtz treatment. Scale bar = 100 μm.

While we could not detect *osx*- or *osc*-driven fluorescence in Mtz-treated fin tissue, we cannot exclude the possibility that a small number of fin osteoblasts were spared. To confirm depletion of fin osteoblasts, we performed flow cytometry on caudal fin tissues of *osx:NTR*; *osc:EGFP* fish that had been treated with vehicle or Mtz (Figure 8A, B). Mtz treatment decimated the *osc:EGFP*+ cell population, yielding fins with no significant difference in *osc:EGFP*+ events from non-transgenic animals (Figure 8C). Thus, we created a system that permitted massive depletion of virtually all adult zebrafish fin osteoblasts.

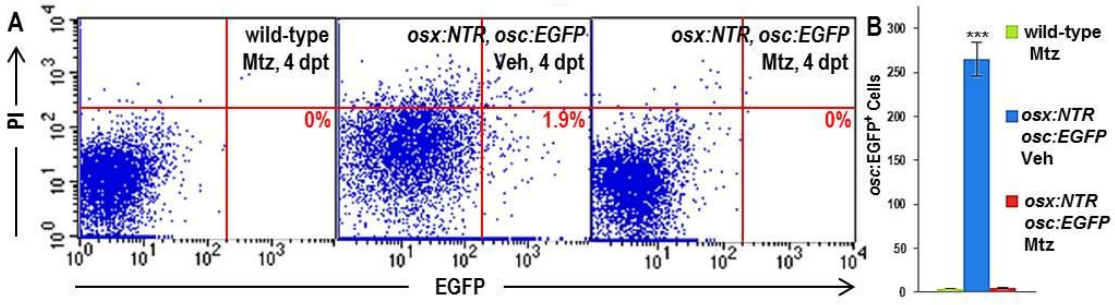

Figure 8: FACS Analysis Confirms Complete Ablation of Osteoblasts

(A) Flow cytometric analysis of caudal fin cells from wild-type (non-transgenic) and *osx:NTR; osc:EGFP* fish treated with vehicle or Mtz. Single cell suspensions were stained with propidium iodide (PI) and analyzed for EGFP. Numbers in the lower right box indicate relative percentages of *osc:*EGFP^{+} cells. **(B)** Absolute *osc*:EGFP cell counts (per 10,000 cells) from data in (C). Data are mean ± SEM from 9 animals each. ***$p < 0.001$, Student's t-test. Wild-type and Mtz-treated *osx:NTR; osc:EGFP* samples show no significant difference in *osc:*EGFP^{+} cells, indicative of complete osteoblast loss.

To determine the longer term consequences of this procedure, we followed *osx*-driven *mCherry-NTR* fusion protein and *osc:EGFP* fluorescence after Mtz treatment. *osx:NTR*; *osc:EGFP* caudal fins began to recover osteoblast marker expression by 7 dpt, with virtually complete restoration by two weeks (Figure 9). Our results indicate that zebrafish regenerate their fin osteoblast compartment within two weeks of its genetic depletion.

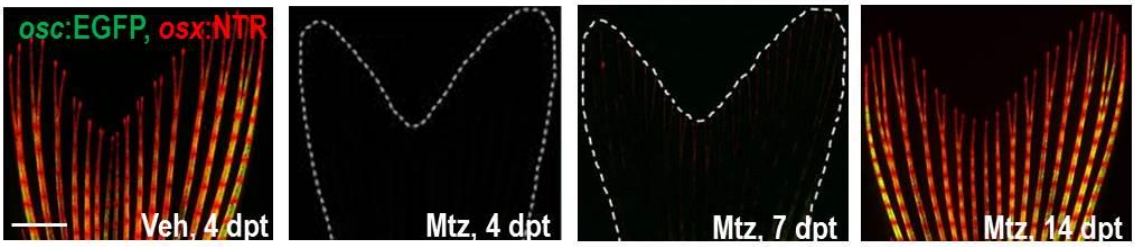

Figure 9: Recovery of Fin Osteoblasts After Genetic Ablation

Caudal fins of *osx:NTR; osc:EGFP* fish lose osteoblast fluorescence within 4 days of Mtz treatment. Expression of *osx*:NTR can be detected beginning at 7 days post-treatment (dpt). Expression recovers completely by 14 dpt (H). Scale bar = 1 mm.

3.1.4 Normal Regeneration of Amputated Fins in Ablated Zebrafish

To examine whether regeneration of amputated fins can initiate and progress without a notable source of bone, we treated *osx:NTR* fish with Mtz or vehicle for 24 hours, returned animals to aquarium water for 2 days, visually confirmed loss of transgene fluorescence, and amputated fins (Figure 10).

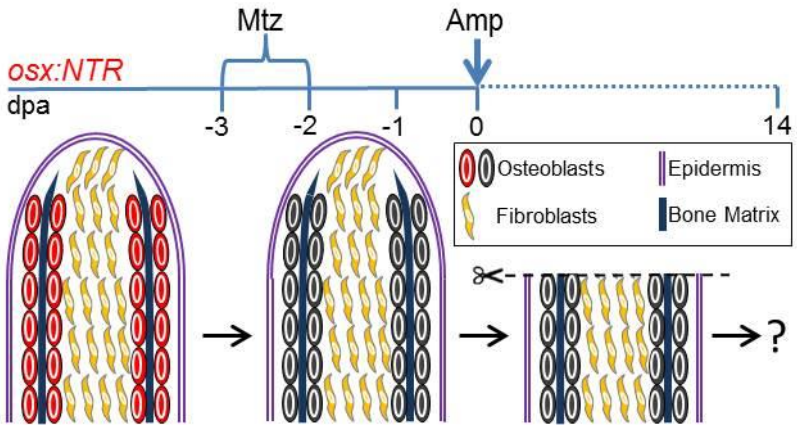

Figure 10: Schematic to Assess Regeneration of Amputated Fins After Genetic Ablation of Osteoblasts

We then imaged and measured fin regenerates every two days after amputation over a course of 14 days. As negative controls, we measured the rate of fin regeneration of wild-type fish treated with Mtz 2 days prior to amputation. Unexpectedly, we observed no significant difference in the rates of regeneration among these three groups at any timepoints (Figure 11A). Importantly, our data indicate that, although osteoblasts in the appendage stump make contributions to regenerated bone, they are dispensable for regeneration of bony fin rays.

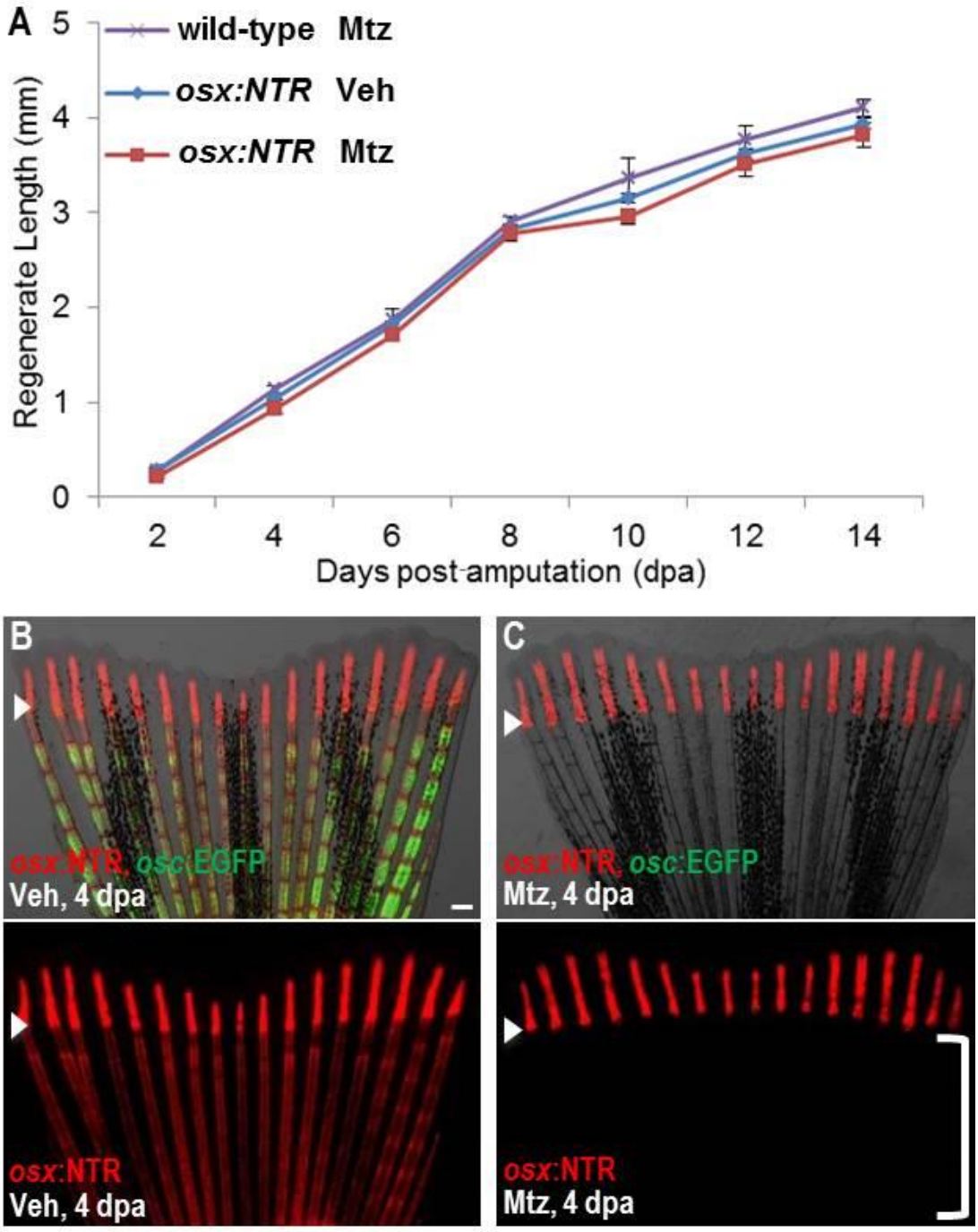

Figure 11: Osteoblast-Depleted Fins Regenerate Normally After Amputation

(A) Lengths of fin regenerates after osteoblast ablation and amputation. As a negative control, wild-type animals were treated with Mtz 2 days before amputation and 4 days after amputation (wild-type, Mtz). *osx:NTR* animals treated with vehicle (*osx:NTR*, Veh) or Mtz (*osx:NTR*, Mtz) prior to amputation regenerated fins with similar efficacy. Data are mean ± SEM from 15 animals each. **(B, C)** *osx:NTR; osc:EGFP* animals had indistinguishable regenerative lengths at 4 dpa whether or not osteoblasts were present prior to amputation, and indistinguishable *osterix*-driven expression in the regenerate. Osteoblast depletion proximal to the amputation plane is evident in Mtz-treated animals by the absence of marker expression (C; bracket). Bottom images show *osx:*NTR fluorescence only. Arrowheads indicate the plane of amputation. Scale bar = 100 μm.

To identify unique developmental responses of osteoblast-depleted fins during regeneration, we analyzed marker expression in *osx:NTR*; *osc:EGFP* animals at various time points post-amputation. Fins from animals treated with Mtz prior to amputation lacked detectable *osx:NTR* fluorescence proximal to the amputation plane at 2-4 dpa, except for a small trail of *osx*-expressing cells at the injury site in 3 and 4 dpa fins. However, they displayed prominent *osx:NTR* fluorescence, indicating that the differentiation kinetics of osteoblasts in regenerating structures were distinct from those in existing fin tissue (Figure 11B, 12). Analysis of sections revealed that recovered *osx:NTR* fluorescence was restricted to the typical osteoblast compartment in the regenerate at 2 dpa (Figure 12A-B, 12G-H). However, by 4 dpa, and occasionally detectable at 3 dpa, *osx:NTR* fluorescence was present in a portion of medially located intraray fibroblasts near the amputation plane of Mtz treated animals only (Figure 12E-F, K-L). These observations of: 1) normal regeneration after massive osteoblast ablation; 2) temporally isolated activation of the osteoblast regulatory program in regenerating tissue versus uninjured areas; and 3) *osterix*–driven expression in medial fibroblast areas, were consistent with existence of an alternative regenerative source to stump osteoblasts.

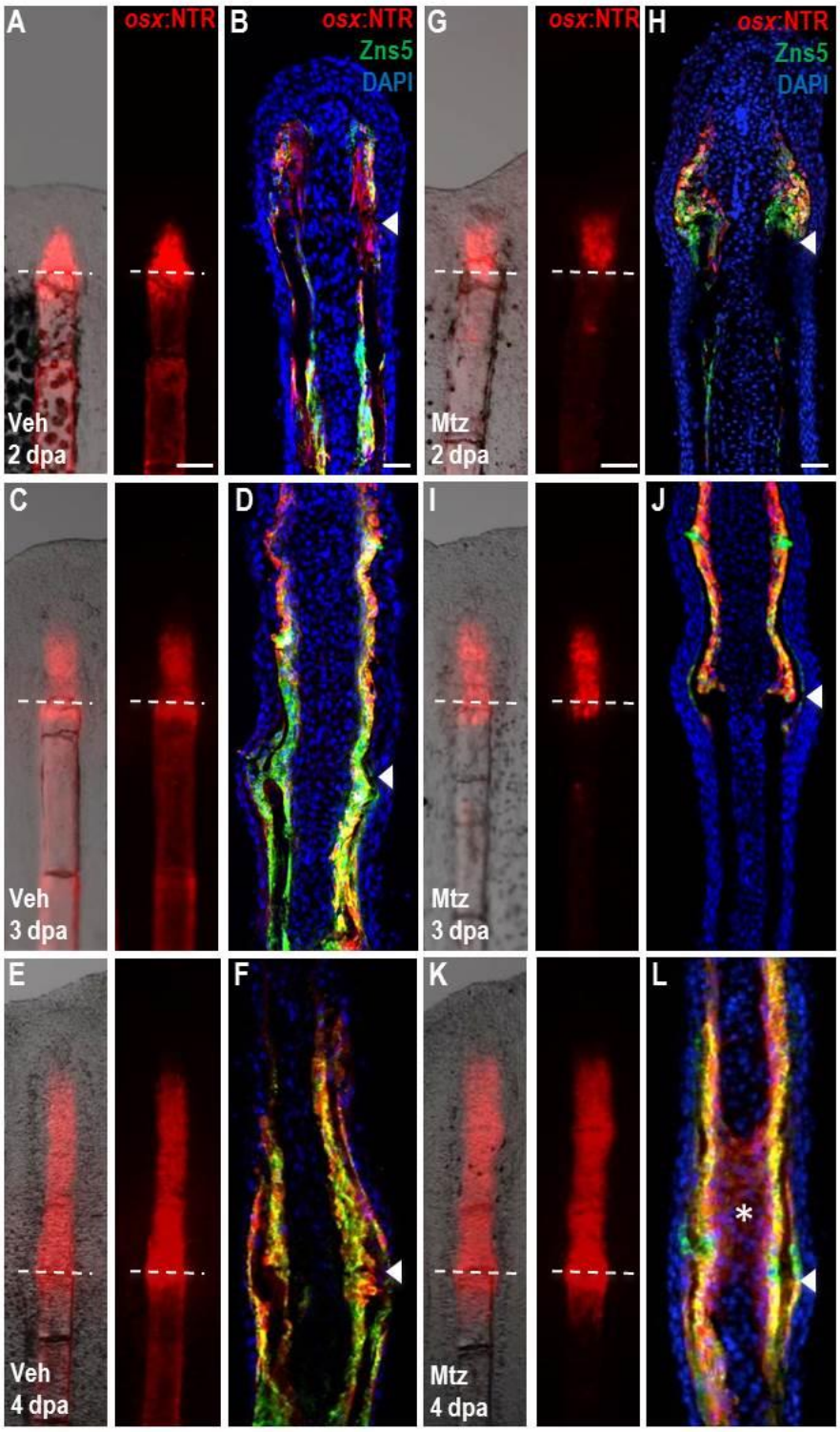

Figure 12: Ectopic *osx* Expression in Osteoblast Ablated Fins

(A-L) Whole-mount views and longitudinal sections of fins at 2, 3, and 4 dpa, highlighting *osterix*-driven NTR fluorescence. *osx:*NTR is undetectable below the amputation plane of fins from Mtz-treated animals at 3 and 4 dpa, except for a trail of fluorescent cells at the amputation site. Tissue sections indicate expression of *osx:*NTR in osteoblasts at each of the 3 time points, and ectopic *osx:*NTR fluorescence in intraray fibroblasts at 4 dpa in the Mtz treated group (asterisk in (L)). Dotted lines and arrowheads indicate the plane of amputation. Scale bar = 100 μm.

3.1.5 Lack of Contribution from Osteoblasts to Fin Regenerate After Ablation of Resident Population

While these findings implicated a non-osteoblast source, it remained formally possible that a portion of existing osteoblasts mimicked ablation by downregulating osteoblast markers upon Mtz treatment, and then recovered to contribute a new pool of osteoblasts to the regenerate. To address this mechanism, we first bathed uninjured *osx:CreER; β-act2:RSG; osx:NTR* animals in 4-HT for 24 hours to tag osteoblasts with an irreversible *β -actin2*-driven label. Two days after genetic labeling, we treated these fish with Mtz for 24 hours, depleting all detectable EGFP fluorescence within 2 days. We then amputated these fins and examined them at 4 dpa for reemergence of *β -actin2*-driven EGFP fluorescence in the regenerate. No EGFP fluorescence was detectable after this protocol (Figure 13, 14).

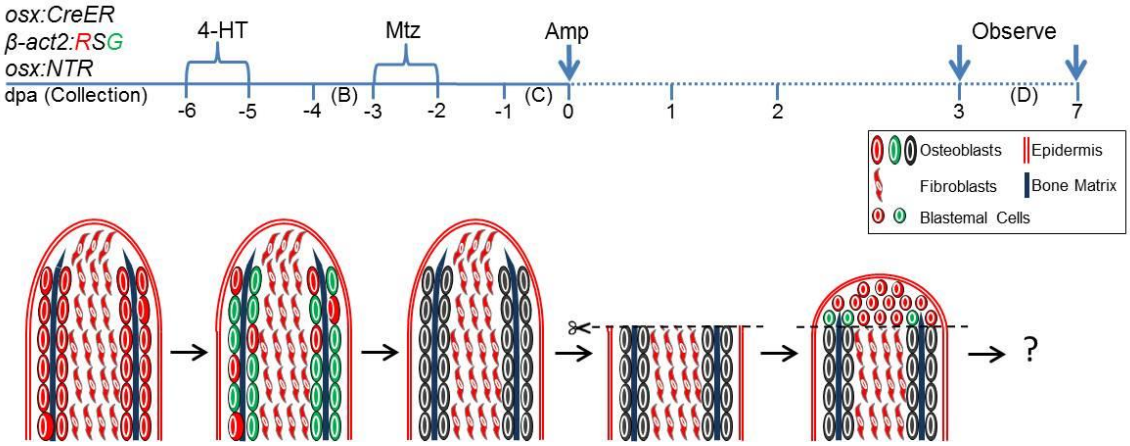

Figure 13: Schematic for Confirming Loss of Osteoblast by Genetic Ablation

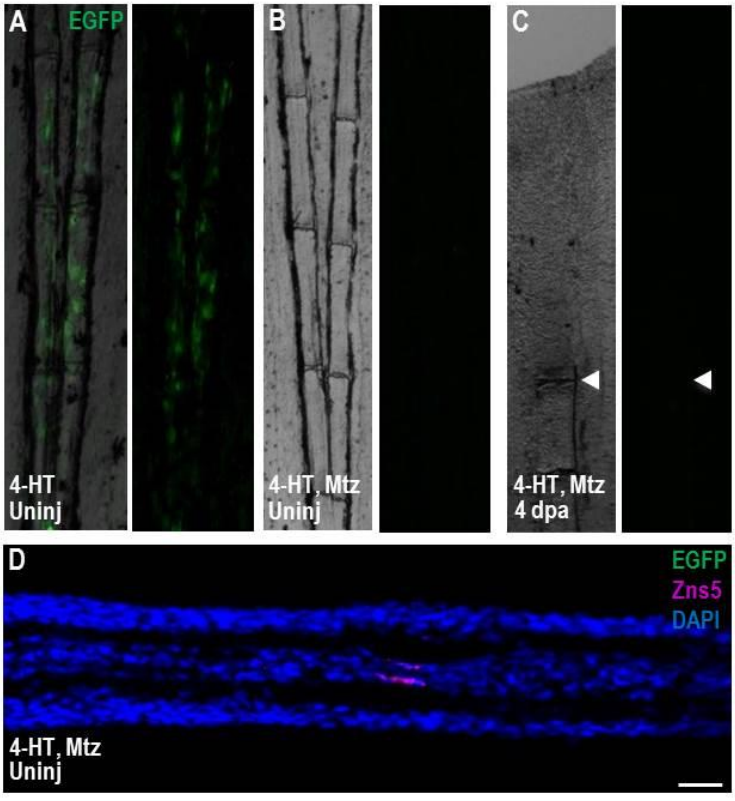

Figure 14: Loss of *β-actin2* Based Label Expression upon Ablation

(A-D) 4-HT labels osteoblasts of uninjured fins with EGFP fluorescence (B). This label was undetectable after Mtz treatment (B), indicating efficient osteoblast ablation.

To confirm these results, we assessed fin samples by cell dissociation and flow cytometry for *β -actin2*-driven EGFP. While uninjured fins from 4-HT-treated animals had many EGFP$^+$ events, Mtz treatment depleted these events to background (EtOH-treated) levels (Figure 15A). EGFP$^+$ events in Mtz-treated fish remained at background levels after amputation and 4 days of regeneration (Figure 15B). These data indicate that no new osteoblasts were contributed to the regenerate from resident *osterix*-expressing cells that had escaped ablation.

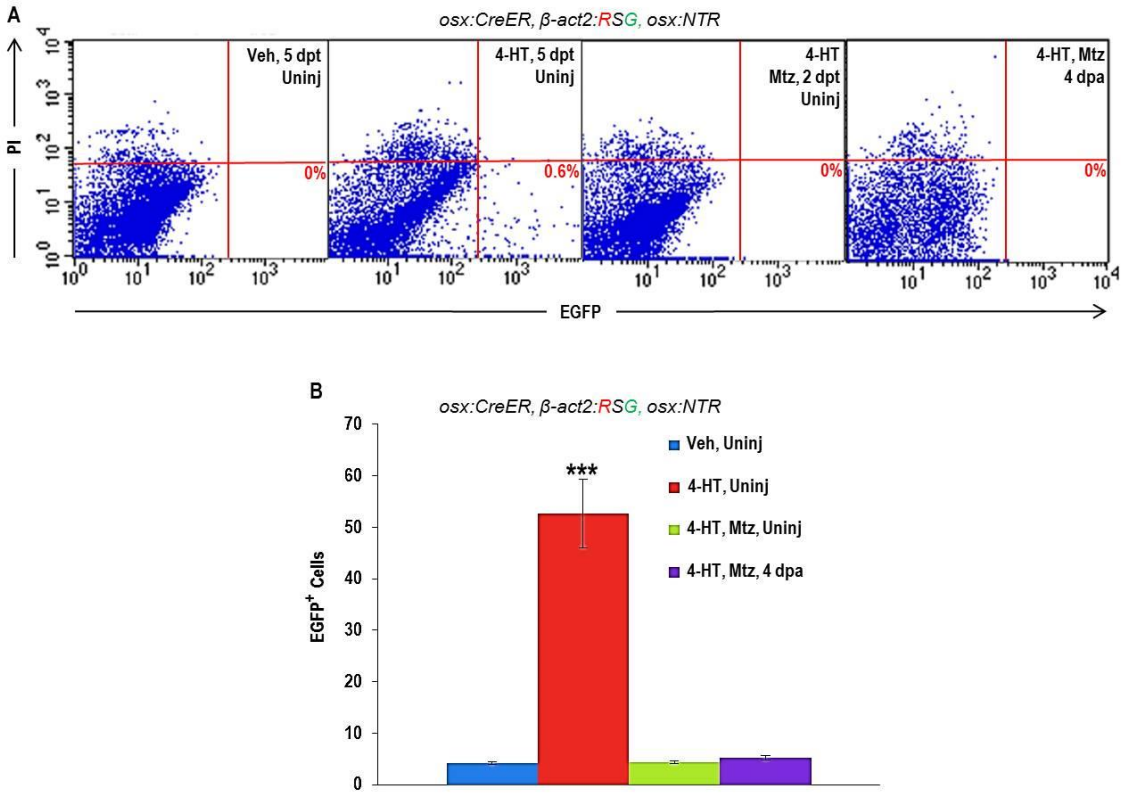

Figure 15: Loss of *β-actin2*-driven EGFP Label After Osteoblast Ablation

(A) Flow cytometric analysis of caudal fin tissues of *osx:CreER; β-act2:RSG; osx:NTR* fish to detect cells expressing EGFP after 4-HT treatment. (Left panels) Fish were treated with either vehicle (left) or 4-HT (left center) and analyzed 5 days post-treatment (dpt). (Right center) An additional group of 4-HT treated fish was bathed in Mtz for 24 hours and analyzed 2 days post-Mtz treatment (dpt). (Right) A last group of 4-HT treated fish was bathed in Mtz for 24 hours, amputated and analyzed at 4 days post-amputation (dpa). Single cell suspensions were stained with propidium iodide (PI) and analyzed for EGFP. Numbers in the lower right box indicate relative percentages of $EGFP^+$ cells. **(B)** Absolute $EGFP^+$ cell counts (per 10,000 cells) from data in (A). Data are mean ± SEM from 9 animals each. ***$p < 0.001$, Student's t-test. Many cells were labeled by 4-HT in these experiments. However, fin samples from 4-HT-labeled animals treated with Mtz show no significant difference in $EGFP^+$ cell numbers from fin samples of vehicle-treated animals. Thus, Mtz treatment effectively depleted cells in the uninjured fin that had been labeled with *β-actin2*-driven EGFP fluorescence through *osx:CreER*, and these cells did not reappear in the regenerate after amputation.

3.1.6 Summary

These findings indicated that existing osteoblasts had been effectively removed by genetic ablation and were not a source of regenerated bone. The data from these experiments suggest that regenerating bone can have a lineage distinct from mature osteoblasts in the appendage stump.

3.2 Molecules Regulating Osteoblast Recovery

3.2.1 In-Situ Screen for Genes Expressed in Regenerating Osteoblast

We undertook a literature survey to obtain list of genes involved in osteoblast or chondrocyte development during mouse limb development. Genes found to be intricately involved in mammalian bone development included the *twist* family (Karsenty, 2008; Karsenty et al., 2009; Kronenberg, 2004; O Rourke and Tam, 2002). *twist* is a is a basic helix-loop-helix transcription factor implicated in osteoblast cell lineage determination and differentiation. It integrates inputs received from various signaling molecules, including *shh* and *fgf* and *BMP* (Hornik et al., 2004; O'Rourke et al., 2002). *twist* expression is required in early stages of bone lineage for commitment and maintenance of immature state: Its loss at late stages of bone development is necessary to achieve terminal differentiation (Bialek et al., 2004; Krawchuk et al., 2010; Kronenberg, 2004; Loebel et al., 2012). Moreover, a zebrafish transgenic line expressing GFP under the control of medaka twist promoter (*oltwist:GFP*) showed induction after fin amputation (Figure 16) (Inohaya et al., 2007). Prior to fin amputation, the fins of *oltwist:GFP* line showed no detectable GFP expression; but at 2 dpa, the regenerate contained several GFP+ cells. Few of these cells co-localized with recovering bone cells. This led us to investigate the expression of twist family and associated genes during zebrafish fin regeneration using in-situ analysis.

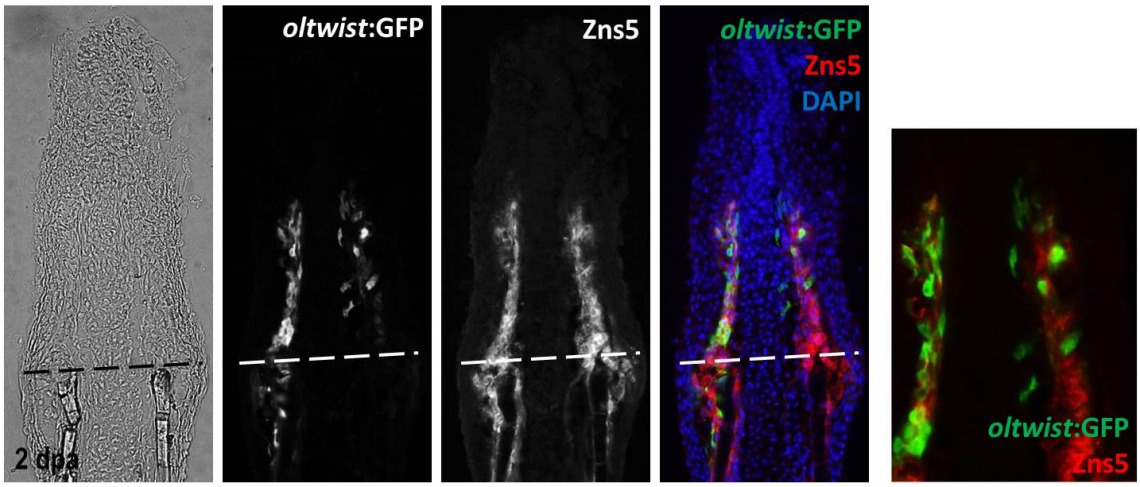

Figure 16: Induction of GFP Signal from medaka *twist* Promoter After Zebrafish Fin Amputation

Expression of GFP fluorescence in a subset of regenerating cells at 2 dpa from the transgenic line *oltwist:GFP*. The region distal to the amputation plane (shown with dotted line) contains most of the cells *GFP*+. Rightmost panel shows a higher magnification of the regenerate with red Zns5 staining, which labels osteoblast cell, and GFP cells. Note co-localization of *oltwist:GFP*+ cells with bone marker.

The in-situ screen carried out revealed two genes with strong expression within the region of recovering bone tissue: *twist3*, a gene belonging to twist family; and *fgfr4*, a fibroblast growth factor receptor (Figure 17). Remaining genes tested in the screen, including *twist* family members (*twist1a, 1b, 2*) and *fgfr* (*fgfr1, 2, 3*), showed expression in epidermis and fibroblast. *twist3* expression by in-situ was strong at 2 dpa; while *fgfr4* in-situ signal was weak, but consistent at 3 dpa.

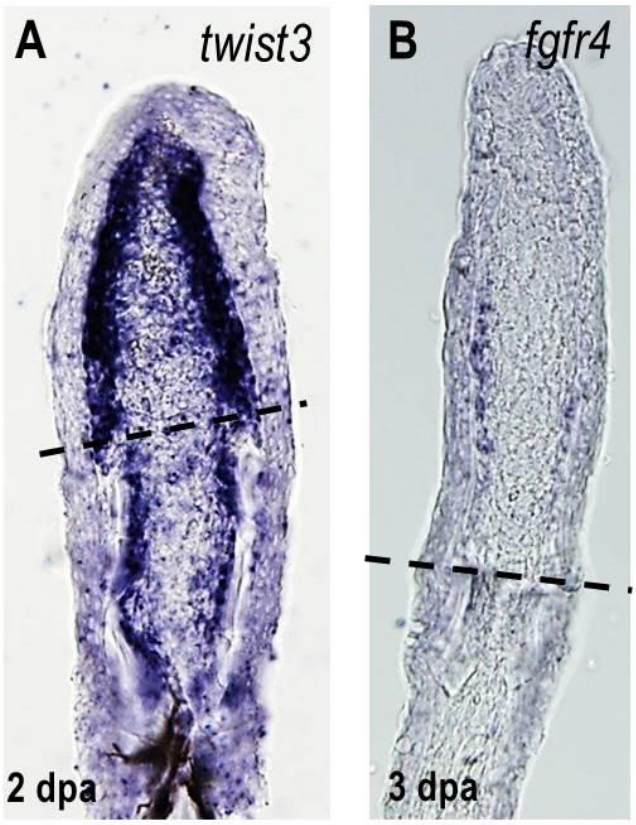

Figure 17: In-situ Screen Isolates *twist3* and *fgfr4*

(A) *twist3* in-situ shows strong signal in the regenerate along the spared bone at 2 dpa. **(B)** fgfr4 in-situ reveals weak signal among the domain of recovering osteoblasts. Dotted line marks the amputation plane.

3.2.2 Transgenic Tools for Visualization of Target Genes

In order to validate the in-situ results, transgenic tools reporting gene activity for *twist3* and *fgfr4* were generated. In addition to confirming expression data, transgenic animals provide an opportunity to study gene regulation in a dynamic fashion at a higher resolution. *HA-twist3* and *fgfr4:EGFP* zebrafish were generated to achieve such goals.

3.2.2.1 Knock-in of HA Epitope Tag into Endogenous *twist3* gene

To observe *twist3* dynamics at cellular resolution during fin regeneration, an in-vivo label of gene promoter or gene product was needed. Promoter driving fluorescence expression was not possible due to lack of BAC containing *twist3* gene along with the DNA sequences surrounding *twist3* in the current zebrafish genome annotation. The absence of regulatory sequences restricted our options to generation of endogenous fusion protein with homologous recombination using available cDNA sequence.

Recently, sequence based editing of specific locations within the genome has been made possible by multiple tools (Gaj et al., 2013). These tools include Zinc Finger Nuclease, transcription activator-like effector nucleases (TALENs), and clustered regulatory interspaced short palindromic repeat (CRISPR). All the above tools utilize engineered sequence-specific DNA-binding domains fused to a nonspecific DNA cleavage module. The anchoring of nuclease at specific location by the DNA-binding domains produces double strand break at the particular site. DNA double-strand breaks stimulate the cellular DNA repair mechanisms, including error-prone nonhomologous end joining (NHEJ) and homology-directed repair (HDR). The former can be utilized to introduce random mutations at the targeted locus (Carlson et al., 2012; Dahlem et al., 2012; Hwang et al., 2013; Mali et al., 2013); while the latter can be used together with a single strand DNA template to insert required DNA sequences at the repair site (Bedell et al., 2012; Ran et al., 2013).

Insertion of an epitope tag within the twist3 gene to create fusion proteins was achieved by developing TALENs capable of introducing double strand break at the required site. The site for insertion was chosen based on the following three criteria:

1. The insertion site must lie in an area with the least conservation among *twist3* sequences obtained from various species (Figure 18).
2. The modification should remove or introduce a restriction enzyme site for the ease of screening (Figure 20A).
3. Epitope tag-*twist3* fusion should not destroy protein localization (Figure 19).

To find the site of least conservation within *twist3* protein, all *twist3* DNA sequences present in NCBI database were obtained. The sequences were translated into corresponding protein sequences and aligned using ClustalW2 (Goujon et al., 2010; Larkin et al., 2007). The multiple sequence alignment showed high conservation in the basic Helix Loop Helix (bHLH) region (red box, Figure 18), as expected, and also among amino acids C-terminal to bHLH. However, the region N-terminal to bHLH was found to be highly dynamic. In addition, published reports on the subcellular localization of twist protein suggest the 'RKR' motif (blue box, Figure 18) to be required for nuclear localization (Singh and Gramolini, 2009), necessary for function of all transcription factors. Thus, the region N-terminal to the 'RKR' motif was narrowed down for the targeting of epitope insertion.

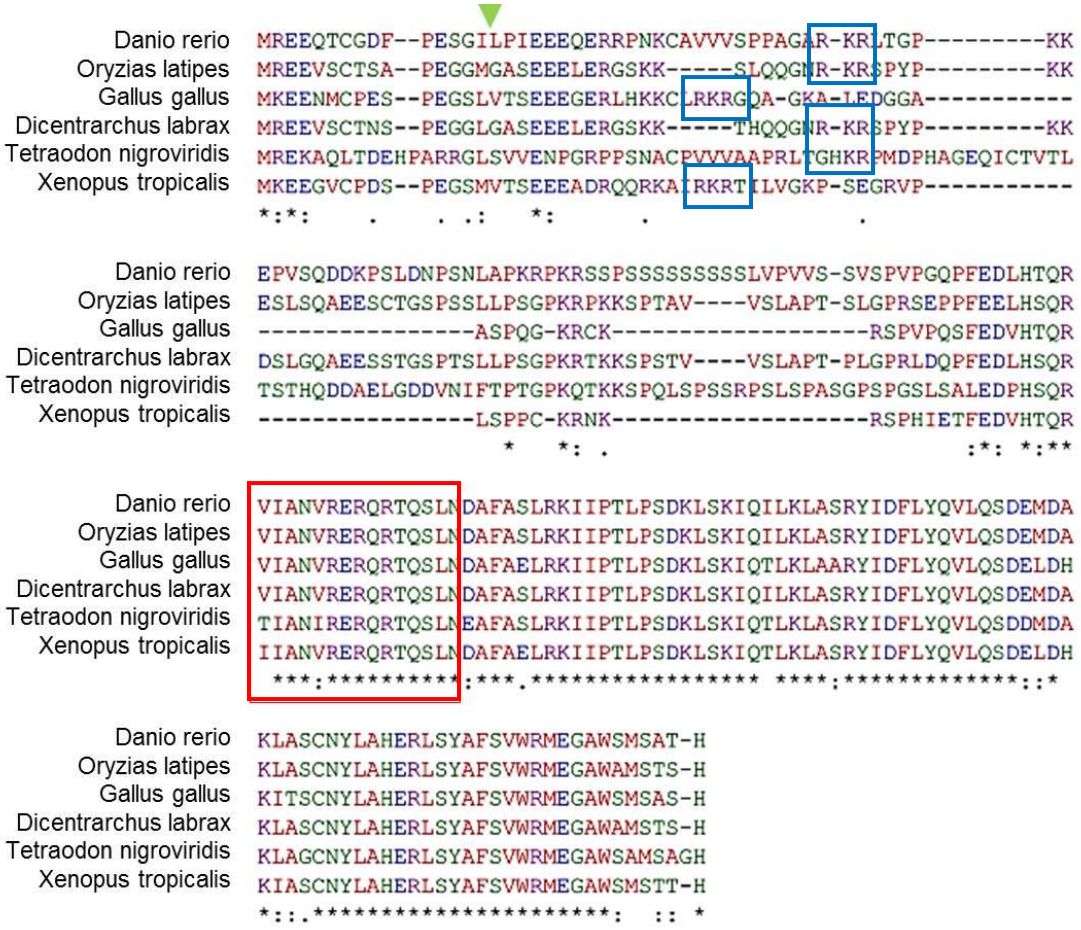

Figure 18: Comparative Analysis of Available *twist3* Sequences Helps Isolate Site of Epitope Insertion

Sequence Alignment of multiple *twist3* genes found in NCBI database using ClustalW2. Genes belonged to a range of species, including fish: Zebrafish (*Danio rerio*), Medaka (*Oryzias latipes*), European seabass (*Dicentrarchus labrax*), Green spotted pufferfish (*Tetraodon nigroviridis*); birds: Chicken (*Gallus gallus*); and amphibian: Western clawed frog (*Xenopus tropicalis*). Red box donates basic Helix Loop Helix domain, blue box the nuclear localization sequence. Green arrowhead donates the epitope tag insertion site.

The DNA sequence corresponding to the region N-terminus to nuclear localization sequence was digested with NEBcutter to reveal presence of restriction sites. *BamHI* restriction site (GGATCC) was found in this region (Figure 20A). This site was selected for targeting by TALENs for generation of *twist3* mutants and insertion of epitope tag. The modification of sequences at this location would destroy the *BamHI* restriction site, whose loss can be easily accessed by PCR amplification of *twist3* gene followed by restriction digestion. This allows rapid and inexpensive identification of modified fish.

The utilization of *BamHI* site required one last criterion to be fulfilled: the fusion protein should not destroy *twist3* subcellular localization. To confirm nuclear localization of fusion protein, we fused the HA epitope tag inserted in frame at *BamHI* site within *twist3* cDNA. HA epitope tag was selected due to the lack of background signal upon antibody staining in wild-type zebrafish embryo (Figure 19, lower panel). HA tag *twist3* fusion (*HA-twist3*) mRNA was transcribed in-vitro and injected into single cell stage zebrafish embryo for production of fusion protein. Antibody staining revealed nuclear localization of *HA-twist3*, thereby confirming the preservation of proper subcellular localization activity (Figure 19).

BamHI restriction site in the N-terminus of *twist3* gene was chosen for targeting by TALEN. TALEN mRNA injection into zebrafish embryos showed efficient loss of *BamHI* digestion (Figure 20).

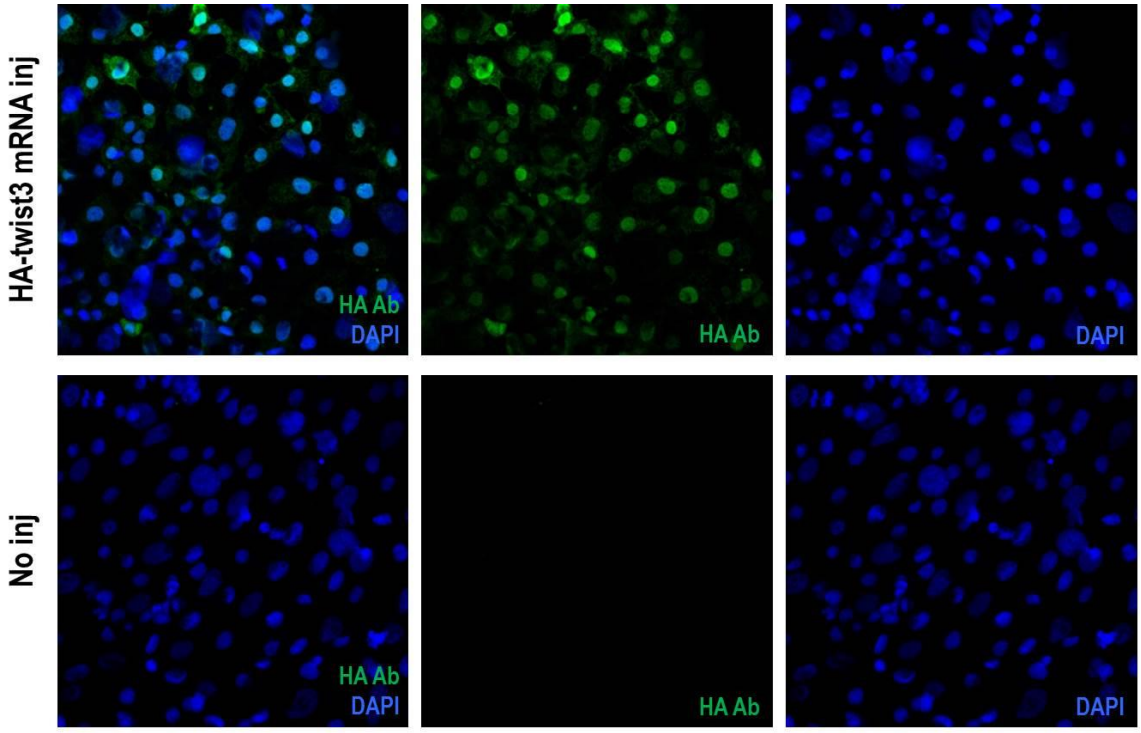

Figure 19: *HA-twist3* Fusion Protein Faithfully Localizes to the Nucleus

HA-twist3 fusion mRNA was synthesized in-vitro and injected into one-cell stages zebrafish embryos. Antibody staining against HA epitope tag was performed on injected (top) and un-injected control embryos (bottom). No background signal could be detected in control embryos, while fusion mRNA injected embryos showed antibody signal in all cells, predominantly localized in the nucleus.

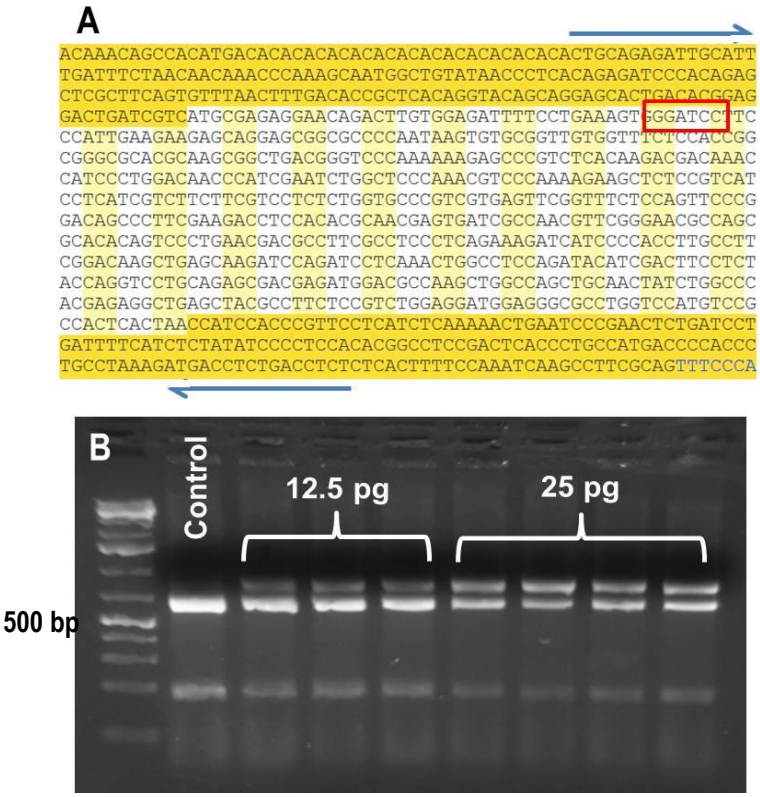

Figure 20: TALENs Targeting *BamHI* Restriction Site Within *twist3* Gene Efficiently Generate Mutations

(A) *twist3* genomic sequence with UTR in dark yellow and cDNA marked with stripes of white and yellow (each stripe represents a codon). The gene has no intron within the coding region. Blue arrows within the UTR depict the location of PCR primers utilized to PCR amplify the gene from the genome. Red Box denoted *BamHI* site. **(B)** Agarose gel with PCR fragments amplified from single embryos that were un-injected (control) or injected with TALEN mRNA, and subsequently digested with *BamHI*. *BamHI* digestion produces bands of two sizes, 560 bp and 190 bp. Presence of undigested band of 750 bp suggests introduction of mutations at the site of restriction enzyme digestion.

Injection of single strand DNA (ssDNA) containing the HA-epitope tag sequence flanked by sequences homologous to double strand break site leads to homology-directed repair with ssDNA as the template, thereby inserting HA epitope tag into the genome. The schematic for isolation of homozygous *HA-twist3* knock-in line is outlined in Figure 21. The TALEN + ssDNA injected embryo are raised to adulthood and mated with wild-type fish to generate families with potential germline founders (blue stripes fish in Figure 21). The founders in F1 generation are isolated by extracting DNA from fin clips and performing PCR amplification of *HA-twist3* gene using HA-specific FP and *twist3*-specific RP. A positive band is only possible upon insertion of HA sequences into *twist3* locus. The complete *twist3* gene is cloned and sequenced to verify precise insertion. Positive *HA-twist3* F1 fish are mated to wild-type fish to generate family with multiple tagged fish. *HA-twist3* knock-in male and female from F2 family are mated to each other to obtain homozygous animals (uniform blue color fish in Figure 21). Homozygous insertion is verified by digesting PCR amplified *twist3* locus with *BamHI*; since homozygotes give no *BamHI* digested band due to destruction of the site by insertion of HA epitope tag.

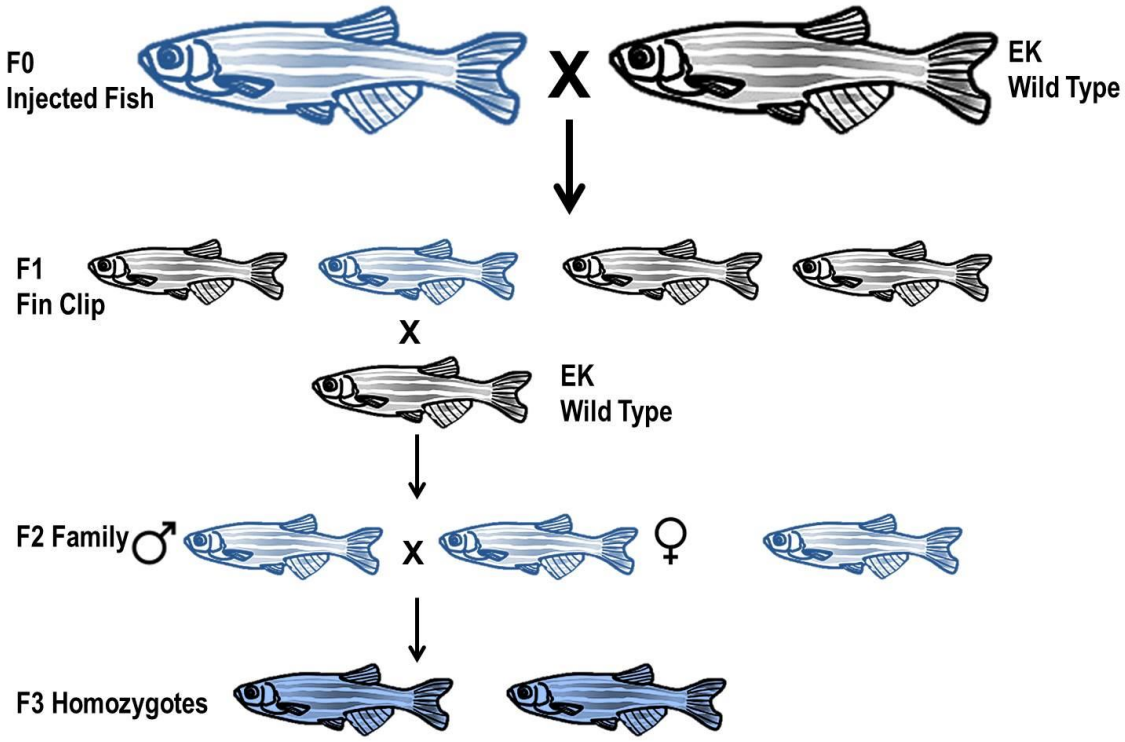

Figure 21: Schematic to Isolate Homozygous *HA-twist3* Fish

To observe *twist3* expression pattern during fin regeneration, amputated caudal fins from homozygous *HA-twist3*, *osx:mCherry* fish were collected at 2 dpa and stained with antibody against HA-epitope tag (Figure 22). Antibody staining showed *HA-twist3* protein localized to the nucleus of cells extending along the spared fin rays and meeting at the tip of regenerate. Expression level of *HA-twist3* was highest at the tip, which consists of immature cell types; and decreased towards the amputation plane, where *osx*+ cells are at later stages of osteoblast differentiation. The negative correlation between *twist3* expression level and the state of osteoblast differentiation is consistent

with the role of *twist* from mouse studies in maintaining bone cells in an immature state (Bialek et al., 2004; Komaki et al., 2007).

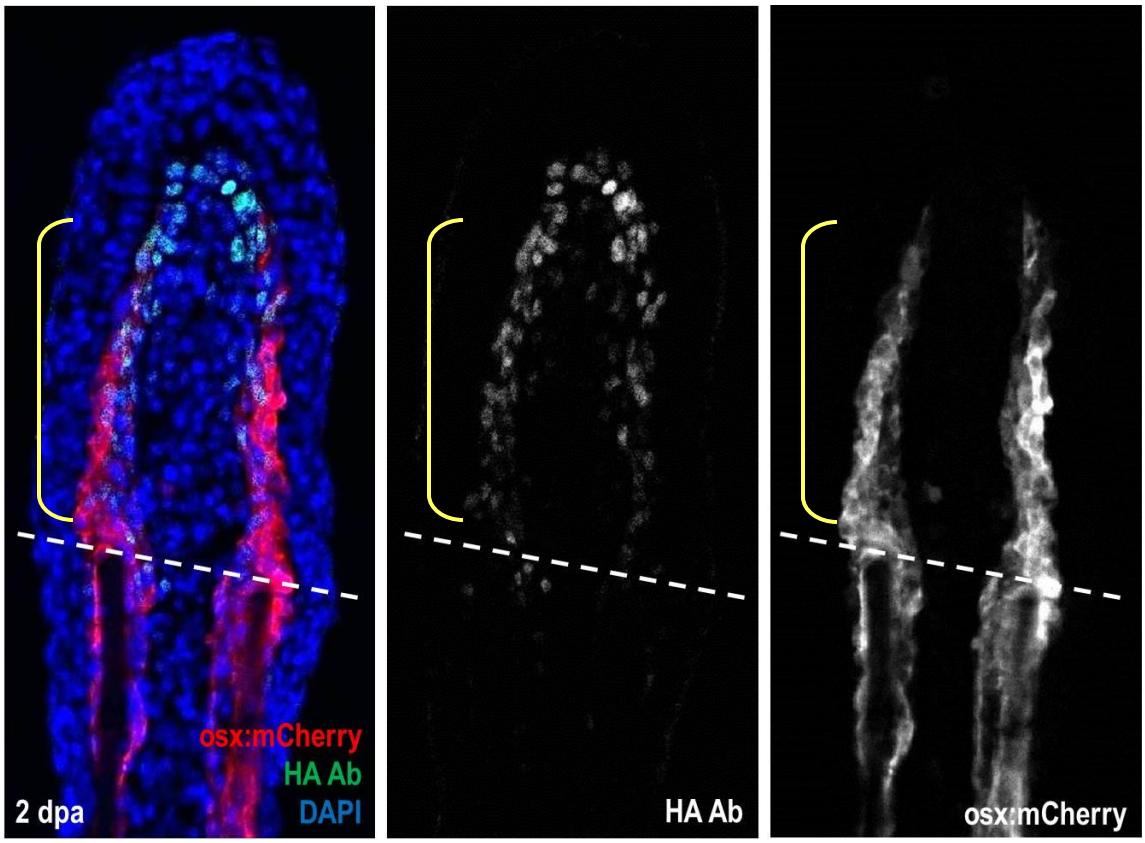

Figure 22: *twist3* is Expressed Within the Recovering Bone Compartment, with the Expression Level Increasing from the Amputation Plane to the Tip

HA-twist3 expressing cells were detected by staining transverse sections across fins from homozygous *HA-twist3, osx:mCherry* with HA-epitope antibody. *HA-twist3+* cells extend along the spared fin-ray and meet at the tip of regenerate. Cells at the tip have highest level of *twist3* expression, but no *osterix* signal; while cells closer to amputation plane with low *twist3* expression level are *osx:mCherry+* (yellow bracket), suggesting they are in later stages of osteoblast differentiation.

3.2.2.2 Generation and Analysis of *fgfr4:EGFP*

A BAC containing sequences 100 kb upstream and 40 kb downstream of *fgfr4* was obtained and modified to introduce EGFP at the translation start site (ATG) of fgfr4 coding sequence (Figure 18A). The modified BAC was injected to generate germline founders. Tg(*fgfr4:EGFP)* faithfully recapitulated embryonic expression reported on ZFIN website (http://zfin.org/ZDB-GENE-980526-488), suggesting that *fgfr4:EGFP* can be used to follow gene activity in various biological contexts, including regeneration.

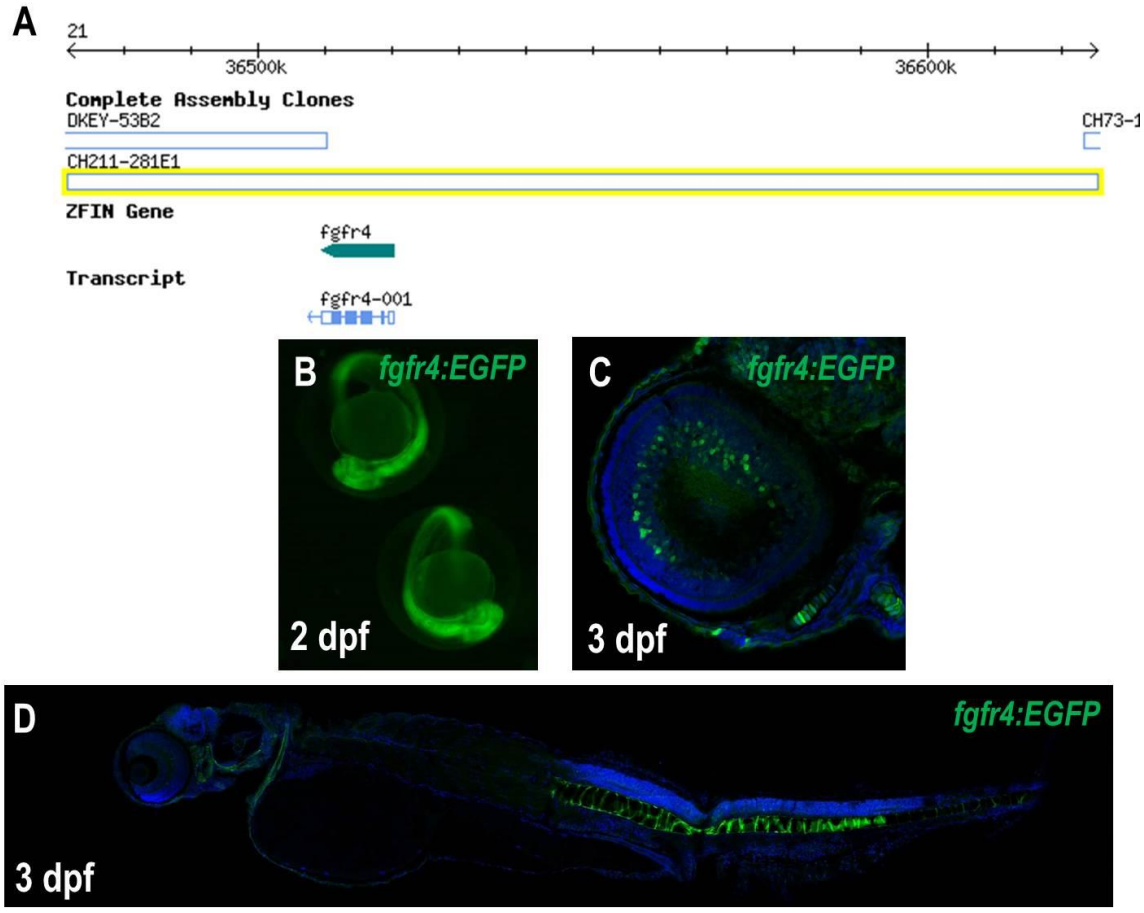

Figure 23: *fgfr4(BAC):EGFP* Line Recapitulates Embryonic Expression

(A) Map of a region of Chromosome 21 within the zebrafish genome, with the BAC containing fgfr4 shown below (marked by yellow boundary.) The BAC, CH211-281E1, contains 100 kb of sequence upstream *fgfr4* and 40kb region downstream *fgfr4*. **(B-D)** fgfr4:EGFP expression at various stages of embryonic development. Ubiquitous expression is detected at 2 dpf. Photoreceptors in eye and notochord show strong expression at 3 dpf.

In adult zebrafish, expression in uninjured fins was found in a subset of cells surrounding fin rays (Figure 19). The cells expressing *fgfr4* co-localized with bone marker *osx*. The strongest and most consistent expression was observed in cells at the edge of semi-circular hemirays. This part of hemi-rays is surrounded by fin fibroblast and is in close proximity with the nervous tissue (the functional significance for such correlation cannot be tested currently). In summary, the osteoblast lineage present in uninjured fin encompasses the *fgfr4* expressing cells.

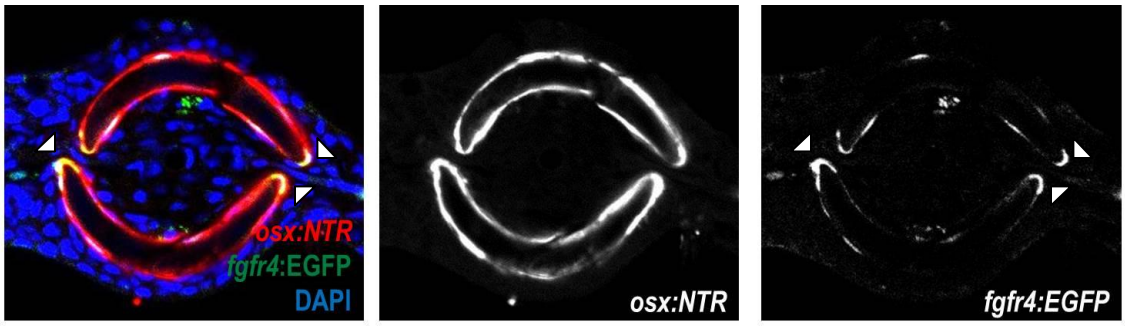

Figure 24: *fgfr4:EGFP* Expression in Uninjured Zebrafish Fins

Transverse section across fin of *fgfr4:EGFP*, *osx:NTR* zebrafish shows co-localization of *fgfr4*+ cells with osteoblasts. *fgfr4* expressing cells were consistently located at the edge of hemirays (arrowheads).

After fin amputation, *fgfr4* expression was investigated, in background of *osx:mCherry-NTR* osteoblast reporter line, at 3 dpa (Figure 20A). At this time point, *fgfr4:EGFP*+ cells were detected in the regenerate within the recovering osteoblast compartment, thereby validating the in-situ result and confirming that *fgfr4*+ cells are restricted to bone lineage. The time point of 3 dpa corresponds to the presence of dedifferentiated osteoblasts in the regenerate and highest levels of cell proliferation in the fin (Knopf et al., 2011). The expression of an *fgf* receptor in the recovering bone cells might suggest possible role in enhancing proliferative capacity as a response to injury.

To further confirm restriction of *fgfr4* expression to cells committed to the osteoblast lineage, bone cells were ablated by Mtz treatment of *fgfr4:EGFP*, *osx:mCherry-NTR* fish and fins amputated 2 days after treatment. In this scenario, de novo osteoblasts are detected by 2 dpa, which subsequently proliferate to repopulate the bone tissue. *fgfr4:EGFP* expression at 3 dpa was again restricted to *osx*+ cells within the regenerate (Figure 20B).

In summary, *fgfr4* expression is confined to the osteoblast lineage within the adult zebrafish fin.

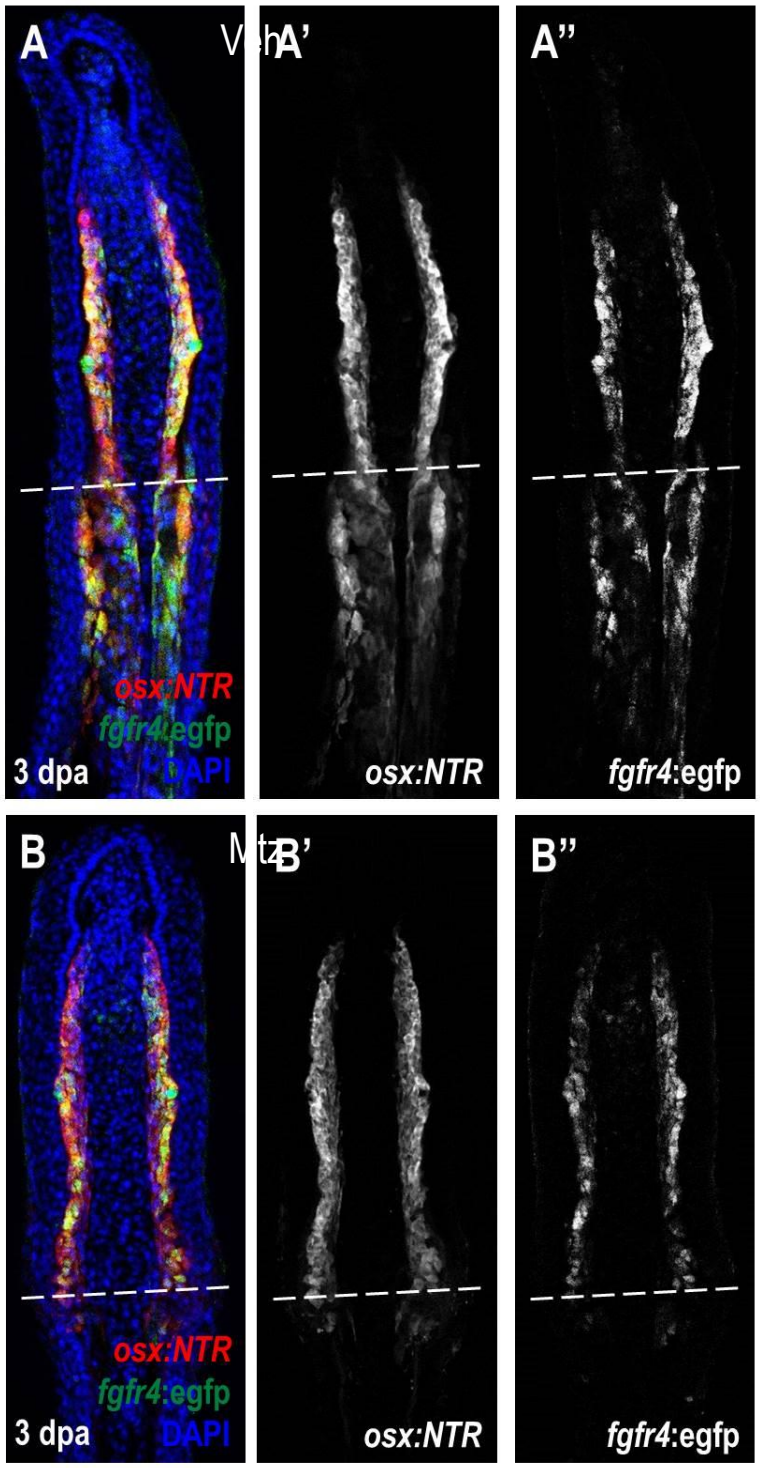

Figure 25: ***fgfr4:EGFP*+ Cells are Restricted to Osteoblast Lineage**

(A) Sections demonstrating *fgfr4:EGFP, osx:mCherry-NTR* fin expression at 3 dpa. Co-localization of EGFP and mCherry expression indicates expression of *fgfr4* within bone tissue. **(B)** Fins collected from fish treated with Mtz to ablate pre-existing osteoblasts show osteoblast recovery distal to the amputation plane (marked by dotted lines), with these cells expressing *fgfr4* reporter.

3.2.3 Loss-of-function Reagents to Study Role of *twist3*

To investigate the role played by twist3 during fin regeneration, loss of twist3 gene activity was achieved by morpholino (MO) injection and generation of null mutants. Recently, the MO technology has been optimized for in vivo delivery, by covalently linked delivery moiety, which enables cell penetration (Morcos et al., 2008). We used vivo MO to block translation of the transcripts encoding the *twist3* by injection into the dorsal half of fin regenerates at 2 dpa. The remaining ventral half of the regenerate served as internal control tissue. The effects of MOs were assessed at 24 hours post-injection (3 dpa) by comparison of the outgrowth size of the injected and non-injected fin halves. Fin tissue injected with vehicle displayed nearly normal outgrowth compared with the non-injected regenerate (Figure 26). This suggests that MO-mediated knockdowns of *twist3* impair fin regeneration.

The MO used in the study to inhibit *twist3* function has been previously shown to have no effect on embryonic development (Yang et al., 2011). This suggests the role of *twist3* is redundant during development, but required during fin regeneration.

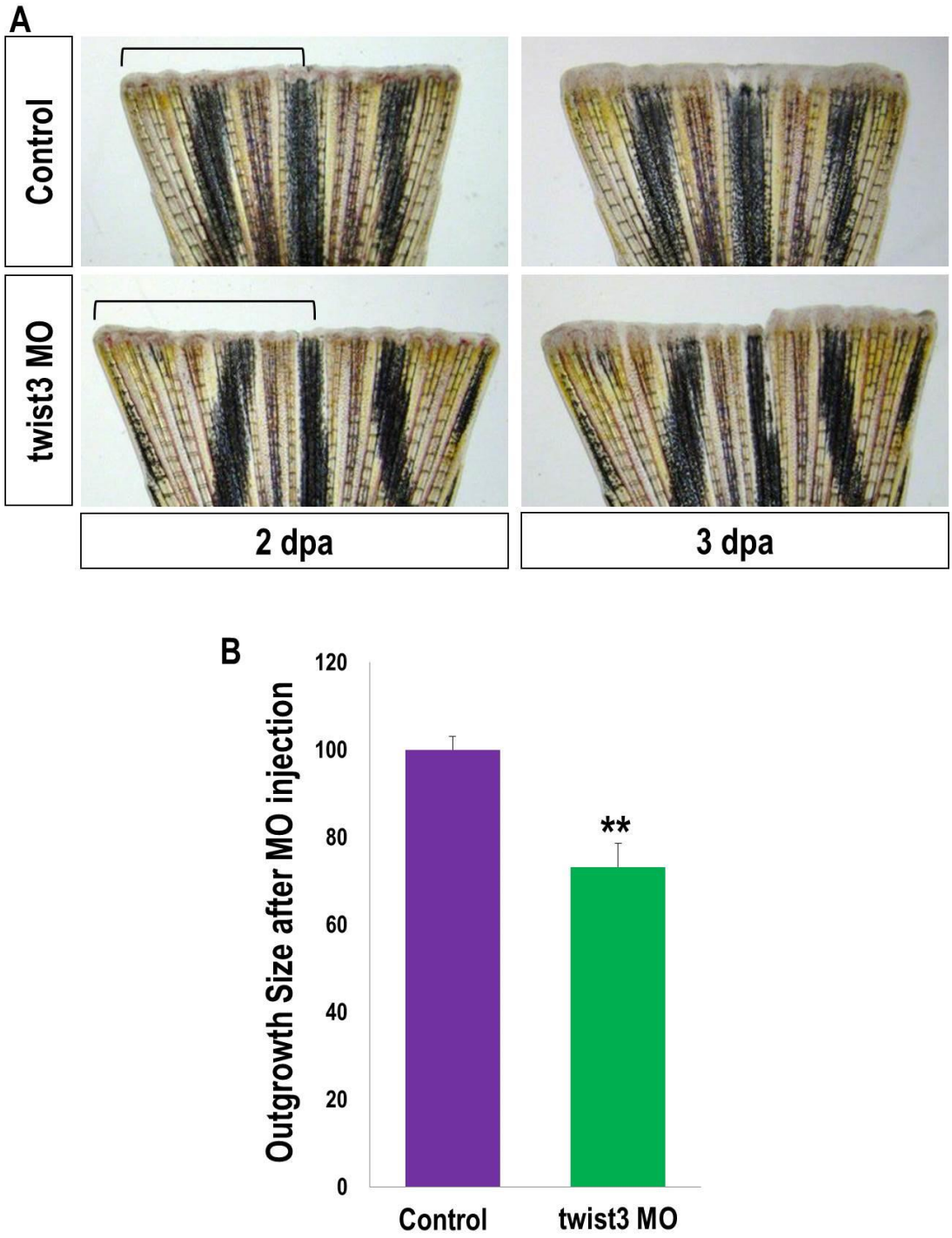

Figure 26: Vivo MO Mediated Knockdown of *twist3* Impedes Fin Regeneration

(A) Fin images of the same fish taken at 2 and 3 dpa. Dorsal half of the caudal fin were injected at 2 dpa with vehicle (Control) or Vivo Morpholino (MO) complementary to *twist3* start site. Ventral half of fin served as an internal control. At 3 dpa, the dorsal half of fin injected with *twist3* vivo MO showed defective regeneration. **(B)** Quantification of the regeneration block with injection of *twist3* vivo MO compared to control injection. Fin recovered to 76 ± 6% of the expected size with inhibition of *twist3*.

The MO technology has certain drawbacks: injection of MO is an invasive process; MO may have off-target effects; MO based knock-down is not complete. To achieve complete loss of *twist3* function without off-target effects or invasive manipulation of fin tissue, a genetic null mutant is required. The survival of *twist3* null mutant to adulthood could be possible due to the lack of embryonic phenotype from MO injection (Yang et al., 2011). Mutations at *twist3* locus to generate null mutant were obtained by injection of TALENs alone. At almost 10% frequency, TALENs induced germline transmittable mutations at *BamHI* site in *twist3* gene. Using the scheme outlined in Figure 21, three *twist3* mutant heterozygotes were isolated (Figure 27). All three mutants have a truncation of *twist3* gene due to the codon TGA coming in frame with start codon. We are currently crossing the heterozygotes with each other to generate null mutants, which will be useful to study the role of *twist3* in greater detail.

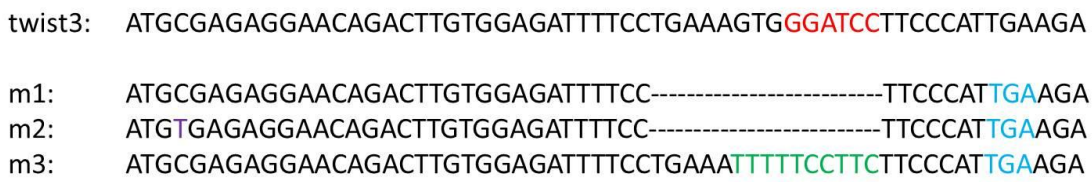

Figure 27: Nature of *twist3* Mutants Isolated

The start of *twist3* coding sequence is shown at top. GGATCC in red represents the *BamHI* site that was used to screen for mutation of twist3 genetic locus. Three separate mutants were isolated from pool of adult F1 fish, depicted by m1-3. All three lose *BamHI* site. m1 has a loss of 14 bp. m2 lacks same 14 bp, but also has a C -> T nucleotide change at 4th position (shown in violet color). The C -> T conversion could be a natural SNP, and not a result of TALEN targeting. In m3 mutant, 9 bp including *BamHI* site is converted to 10 bp random sequence (in green). In all three cases, the codon TGA (in blue) shifts in frame with translation start ATG and encodes for the STOP codon, thereby truncating *twist3* gene and removing all functional elements.

3.2.4 Summary

Fin amputation in zebrafish induces expression of *twist3* within 2 dpa, and of *fgfr4* within 3 dpa in the recovering osteoblast lineage. Expression of *twist3* correlates negatively with the level of osteoblast differentiation. *fgfr4* induction correlates with the time point for highest proliferation in regenerating fin.

4. Discussion and Future Directions

4.1 De Novo Osteoblast Formation

Appendage regeneration has been studied for nearly 250 years, and many hypotheses regarding the source of new tissue have been put forward. Arguments for and against resident stem cells, dedifferentiation and transdifferentiation can be found in the literature. Most of the previous studies relied on morphology to detect cell populations, irradiation and invasive techniques like transplantation; each of these could bias the results towards different source. Only recently have genetic technologies become available to resolve the cellular basis of regeneration in-vivo in a non-invasive manner. Here, a combination of genetic cell ablation and fate-mapping approaches was applied to define the importance of existing osteoblasts in regeneration of the skeletal bone of zebrafish fins. The study, along with other published data, highlights a primary cellular mechanism for bone regeneration in which existing osteoblasts undergo de-differentiation, proliferate, and contribute new osteoblasts (Knopf et al., 2011; Sousa et al., 2011; Stewart and Stankunas, 2012; Tu and Johnson, 2011). In addition, the study adds key context to the results of recent lineage-tracing experiments in regenerating zebrafish fins. The data indicates that such events are dispensable, and that osteoblasts can regenerate readily after amputation through de novo differentiation. Thus, there are multiple cellular sources with the potential to contribute substantially to bone regeneration.

The combination of technologies employed builds upon strategies that have been reported over the past century and have suggested the occurrence of trans-differentiation during skeletal regeneration. In salamanders, new bone can develop in the regenerate after removal of the skeletal elements and subsequent amputation through the affected area (Thornton, 1938). Additionally, although irradiated limbs fail to regenerate after amputation, transplantation of non-skeletal tissues can rescue this capacity (Dunis and Namenwirth, 1977; Namenwirth, 1974). Similar experiments have been performed in teleost fins in which entire fin rays were extirpated before amputation, a manipulation that has multiple interpretations and has yielded mixed results (Goss and Stagg, 1957; Nabrit, 1929; Nabrit, 1931; Turner, 1941). Our approach using genetic tools clearly indicates that non-osteoblast cells can be a primary or exclusive source of new, patterned appendage skeleton.

4.2 Facultative Regeneration?

Recent clonal analyses suggested that osteoblasts are not clonal partners with intraray fibroblasts or other recognized fin cell types during ontogeny or regeneration (Stewart and Stankunas, 2012; Tu and Johnson, 2011). It is possible that a modified clonal analysis approach, employing stable transgenic lines and irreversible labeling (e.g. Cre recombinase technology), would provide new opportunity to represent all fin cells and recognize heterogeneous clone partners (Tanaka and Reddien, 2011). On the other hand, it is possible that osteoblast depletion triggers a novel source that does not normally

participate in regeneration of amputated fin rays, and is thus an example of 'facultative regeneration'. There are precedents for dormant regenerative mechanisms that emerge predominantly in special contexts. For instance, pancreatic β-cells regenerate after resection injury by self-replication (Dor et al., 2004), yet can be replenished by duct cell or α-cell transdifferentiation after injuries of ischemia or extreme β -cell loss, respectively (Thorel et al., 2010). The mammalian liver provides another example for this type of regeneration. If a part of the liver is surgically removed, the remainder proliferates to restore the overall organ size. In this process, the new hepatocytes are formed by division of existing ones. But if the animals have been treated with a drug to suppress division of hepatocytes, then regeneration still takes place, but now the new hepatocytes arise from oval cells, which are small cells lying in the periportal regions that somewhat resemble embryonic hepatoblasts (Alison et al., 1996). Thus, it will be important to determine the extent to which non-osteoblasts contribute bone in the presence of a full complement of osteoblasts, and to identify signals that recognize source availability and regulate output from diverse sources.

4.3 Restriction of Osteoblast Differentiation

During fin regeneration osteoblast are generated in line with the pre-existing bone matrix. Osteoblast generation from a non-osteoblast source also follows the same pattern. This raises the question as to the factors that restrict osteoblast localization. ECM, by itself, may play a role in stimulating osteoblast differentiation. Interestingly,

during fin regeneration osteoblast differentiation zone trails the region of ColX deposition by the epidermis (Figure 28). ColX deposition by chondrocytes in mammalian limb prepares the site for osteoblast ossification (Apte et al., 1992). In the absence of a separate chondrocyte lineage in zebrafish fin, the epidermis might be playing the role of depositing ECM permissive to osteoblast differentiation; and in this manner regulating the region of osteoblasts differentiation.

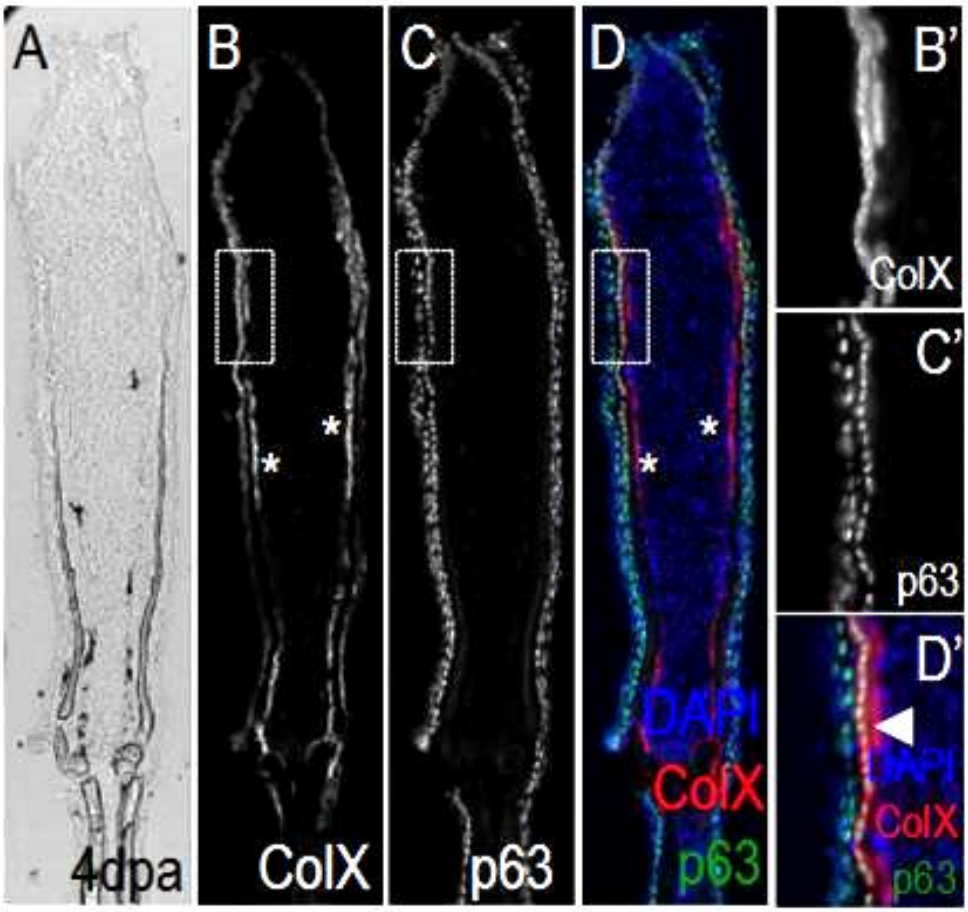

Figure 28: *ColX* Expression in the Epidermis Precedes the Region of Osteoblast Differentiation

(A-D) Transverse section across ColX:mCherry fin rays is stained with p63 antibody to label the epidermis (C, C′). ColX is expressed in the region of bone formation (* in B, D) and also in epidermal cells distal to the differentiation region (inset B′-D′, compare location of inset with * in B, D).

4.4 Determining Contributions from Non-Osteoblast Source

Which cells regenerate bone in the absence of contributions by skeletal osteoblasts? Intraray fibroblasts are the predominant cell type in fins along with epidermis and share with osteoblasts the expression of markers like *msxb*, *msxc* (Figure 29), *sox9a*, and *Col2a1* (Akimenko et al., 1995), genes known in mammals to instruct and/or indicate osteoblast fate decisions (Karsenty, 2008; Karsenty et al., 2009). Thus, they represent primary candidates. Indeed, the ectopic induction of *osterix*-driven fluorescence that we observed in medially located fibroblasts after osteoblast ablation and amputation may be a signature of their trans-differentiation. If the fibroblasts are a bone source in zebrafish, their contributions are analogous to the dermal contributions to cartilage indicated in a recent study of axolotl limb regeneration (Kragl et al., 2009), and suggest an evolutionarily shared regenerative strategy. The use of inducible, Cre-based lineage-tracing experiments is recent to the zebrafish model system, and to our knowledge there is no marker or regulatory sequence with demonstrated specificity to zebrafish fin fibroblasts. Thus, the establishment of new reagents for fate-mapping fibroblasts, as well as other important fin cell types, will advance the findings we report

here. One such tool would be the multi-color clonal analysis (Gupta et al., 2013; Gupta and Poss, 2012; Livet et al., 2007). Conventional clonal analysis using single Loxp based recombination is restricted to fate mapping of the entire population. On the other hand, multi-color lineage tracing, based on stochastic expression of a combination of fluorescent markers, can trace the fate of individual cells within the population. This will allow use of promoters that express in fibroblast as well as osteoblast lineage to drive CreER and label cells uniquely belonging to a particular lineage. Retrospective analysis will allow one to directly test contributions from non-osteoblast source to bone regeneration. Determining the breadth and plasticity of cellular sources in spectacular examples of bone reconstitution like zebrafish fin regeneration stands to illuminate potential therapies of major bone injury or loss in humans.

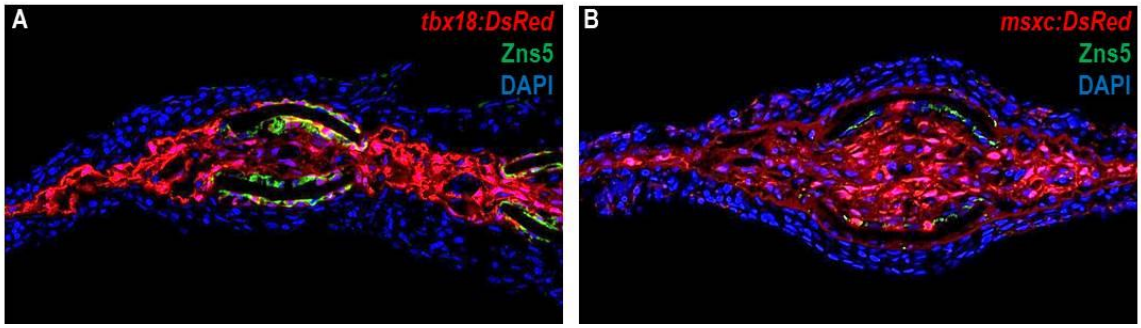

Figure 29: *tbx18:DsRed* and *msxc:DsRed* Show Expression in Both Fibroblast and Osteoblast Lineage

(A-B) Transgenic zebrafish line expressing tbx18:DsRed (A) and msxc:DsRed (B) show fluorescence expression within fibroblasts as well as osteoblasts. Such promoters can be

coupled with multi-color clonal analysis to test contribution from fibroblasts to bone tissue.

4.5 Genes Regulating Maintenance and Proliferation of Immature Osteoblasts

The process of fin regeneration occurs in three phases: wound healing, blastema formation and regenerative outgrowth. Blastema formation requires de-differentiation of spared cells, creating immature cells. The immature cells proliferate to generate enough material to recover the final structure. During the process, the following three conditions need to be fulfilled for successful regeneration:

1. Generation of immature cells (0 – 2 dpa)
2. Maintenance of the immature state until end of regeneration
3. Sufficient amount of proliferation to meet the requirements of lost tissue (highest at 3 – 4 dpa)

Osteoblast recovery in regenerating zebrafish fin occurs from pre-existing osteoblasts. Molecular mechanisms involved in the above three required steps remain unknown. Using hints from mouse limb development literature, an in-situ screen uncovered *twist3* induction at 2 dpa, and *fgfr4* induction at 3 dpa. In-situ result was validated by generation of HA-epitope tag knock-in line for twist3 and BAC based fluorescent reporter line for *fgfr4*. It would be of interest to test the role these genes play during fin regeneration. The working model for their involvement is shown in Figure 30.

In mouse limb development, *twist* gene is required for cells to enter the osteoblast lineage, and its loss is needed for osteoblast cells to terminally differentiate (Bialek et al., 2004; Krawchuk et al., 2010; Kronenberg, 2004; Loebel et al., 2012). The negative correlation of *HA-twist3* expression in regenerating zebrafish fin with the differentiation state of recovering osteoblasts suggests it might play a similar role: maintaining de-differentiated osteoblasts in immature state.

fgfr4 is a receptor for *fgf* signaling, which plays an important role in regulating proliferation of mouse limb bud (Martin, 1998; Niswander et al., 1993; Sun et al., 2002; Vogel et al., 1996). In zebrafish fin, *fgf* signaling instructs position-dependent growth, blastema proliferation, and expansion of fin melanocytes (Lee et al., 2005; Lee et al., 2009a; Lee et al., 2010). Inhibition of *fgf* signaling with a pan-constitutive negative *fgf* receptor blocks fin regeneration completely (Lee et al., 2005); and also deteriorates fin tissue during homeostasis (Wills et al., 2008). Proper *fgf* signaling is necessary for maintenance and regeneration of fin tissue.

Expression of a receptor of *fgf* signaling in recovering osteoblast tissue might make it more sensitive to reception of *fgf* signaling; and thereby increases proliferation rates. This would be an elegant mode of proliferation regulation in a tissue that undergoes low levels of cell division during steady state. *fgfr4* expression regulation might provide temporal control over osteoblast proliferation.

The roles for these genes during fin regeneration will be tested by creation of null mutants. *twist3* heterozygote mutant has been generated, while *fgfr4* mutant is in progress.

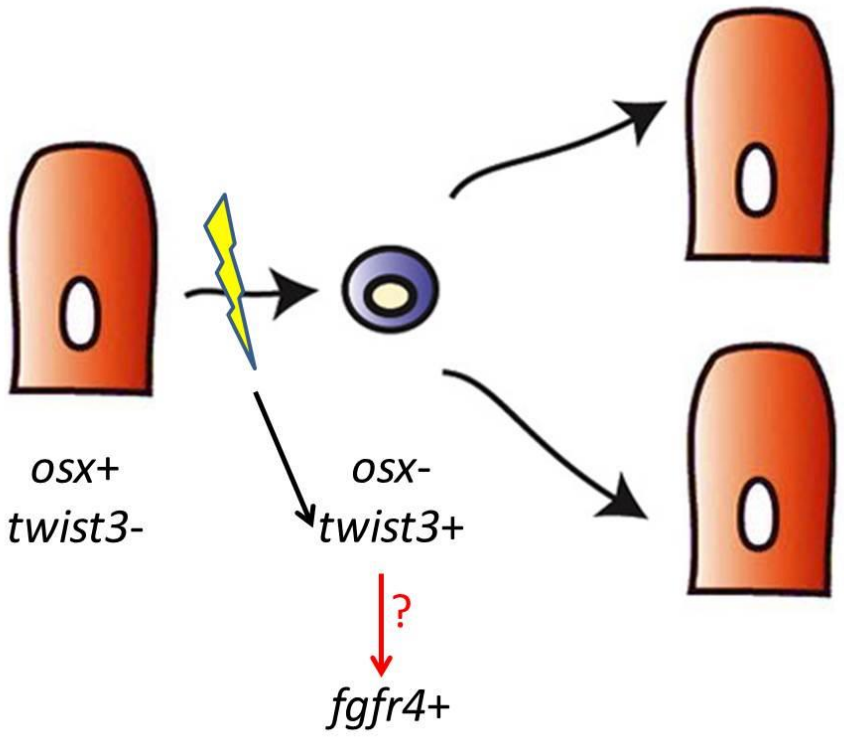

Figure 30: Working Model for Osteoblast Recovery

Cartoon depicting the working model for osteoblast recovery upon fin amputation. Mature osteoblasts are in red and de-differentiated in blue. Spared mature osteoblast expressing *osterix* undergo de-differentiation by 48 hpa. Immature osteoblasts downregulate the expression of *osterix* and induce *twist3* expression at 2 dpa. Subsequently, *fgfr4* expression and proliferation is induced. Osteoblasts proliferation in the regenerate continues until the recovery of final structure.

4.6 Is Regeneration a Recapitulation of Embryonic Development?

Development and regeneration both require generation of a patterned differentiated structure, and thus, may employ the same genetic machinery to achieve their task. However, the zebrafish *devoid of blastema* (*dob*) fin regeneration mutant shows normal development (Whitehead, 2005). *dob* encodes for *fgf20a*, whose loss during development is possibly compensated by *fgf20b*. Similarly, knockdown of *twist3* activity in regeneration zebrafish fin using morpholino antisense technology lead to defective regeneration; but the MO used in the *twist3* experiment has been shown to have no effect of the developing zebrafish embryo (Yang et al., 2011). Thus, regenerative phenomena may employ genes distinct from development.

In spite of the difference in molecules employed during regeneration and development, the genetic network for generation of patterned tissue seems to be shared. The twist family of genes is common to skeleton development and regeneration, with MO based knockdown of *twist1a* or *twist1b* both leading to skeletal defects (Yang et al., 2011). It is possible that in different contexts, the particular players involved in the process are distinct; but the players are related to each other and can probably be interchanged without any noticeable effect.

4.7 Evolutionary Implications of twist3 Involvement

twist3 is one of the four twist genes found in zebrafish. Interestingly, within vertebrates, it is absent in mammals {Germanguz, 2007 #795}. Its homologues have been located in other fish species (medaka, seabass, pufferfish), birds, and amphibians (Figure 18). Recently, *twist3* induction was reported in axolotl upon limb amputation {Kragl, 2013 #393}. Although, *twist3* is up-regulated in two distinct species, zebrafish and axolotl, during appendage regeneration, its presence in genome is not correlated with capacity to successfully regenerate adult limbs. Chicken, which have *twist3*, cannot regenerate limbs. This suggests that loss of *twist3* during evolution is not associated with the loss of regenerative capacity.

This raises the question about the primary role of *twist3* during evolution. If it is osteoblast regeneration, then it is plausible that it interacts with another factor that is specific to regenerative animals and lost in avian and mammalian lineage. On the other hand, utilization of *twist3* in regeneration could be an accidental artifact selected in an ancient vertebrate ancestor. Loss of regeneration in avian lineage may be due to factors not related to *twist3* involvement.

One biological phenomenon is common to all vertebrate lineages that have *twist3* homologue: that of egg-laying. Loss of egg-laying is characteristic of mammals. Interesting, twist mutant in *C. elegans* shows egg-laying defective phenotype {Corsi, 2002

#796}. Analysis of HA-twist3 expression in female zebrafish reproductive system and examining egg-laying behavior in twist3 mutant would be evolutionary importance.

4.8 Determining Genes Regulated by twist3

Highest levels of *twist3* expression occur at 2 dpa, while that of *fgfr4* at 3 dpa. It would be of interest to test the possibility of *fgfr4*, and other genes involved in maintenance of immature state/proliferation, induction by direct binding of *twist3*. The available HA-twist3 homozygous fish provides an opportunity to test this by Chromatin immunoprecipitation (ChIP) using antibody against HA epitope tag.

ChIP allows mapping the positioning of transcription factors on specific genomic regions. In a ChIP assay, DNA and proteins are reversibly cross-linked, chromatin is fragmented, and antibodies to the protein of interest are used to immunoprecipitate a specific protein–DNA complex. Immune complexes are washed, the chromatin is eluted, cross- links are reversed, and the ChIP DNA is purified. Genomic sequences associated with the precipitated protein can be identified by polymerase chain reaction (PCR).

Interestingly, ChIP-chip (Chromatin immunoprecipitation followed by microarray) analysis of twist transcription factor during mesoderm development in *Drosophila melanogaster* (Dm) embryos suggests direct binding of *Dm-twist* to regulatory sequences of *Dm-fgfr* and *Dm-rho* (Zeitlinger et al., 2007). *Rho* is an important component of cell cycle and cell migration machinery, suggesting a role of twist in pattern formation.

As a proof of principle for the possibility of ChIP analysis using the *HA-twist3* reagent, *HA-twist3* mRNA was injected in single-cell embryos and a published protocol (Lindeman et al., 2009) was utilized to perform ChIP experiment at 24 hpf. A well characterized target of twist gene, *periostin* (*postnb*), was utilized for verification (Oshima et al., 2002). 1 kb upstream sequence of *postnb* gene contains six canonical *twist* binding sites (CANNTG, (Ozdemir et al., 2011)) (Figure 31A). The negative control, ubiquitously expressing *β-act2* upstream sequence also contains two twist binding sites (Figure 31B). ChIP using HA antibody, followed by real-time PCR for regulatory fragments containing the *twist* binding sites showed enrichment only for the *postnb* sequence, suggesting binding of *twist3* transcription factor to the promoter of *postnb,* and not *β-act2* (Figure 32).

The experiment suffers from multiple caveats; most importantly from over-expression of *twist3* protein at ectopic locations and in non-physiological amounts. The binding of *twist3* to *postnb* promoter could be a result of high expression level and may not represent physiological situation. Infact, *twist3* could be binding to the sites of other twist family members.

In spite of the drawbacks, the experiment confirms the validity of the tool for the purpose of ChIP analysis. Generation of sufficient amount of adult fin material for immunoprecipitation of DNA quantities that allow deep sequencing will help decipher the genetic network regulated by *twist3* in de-differentiated osteoblasts.

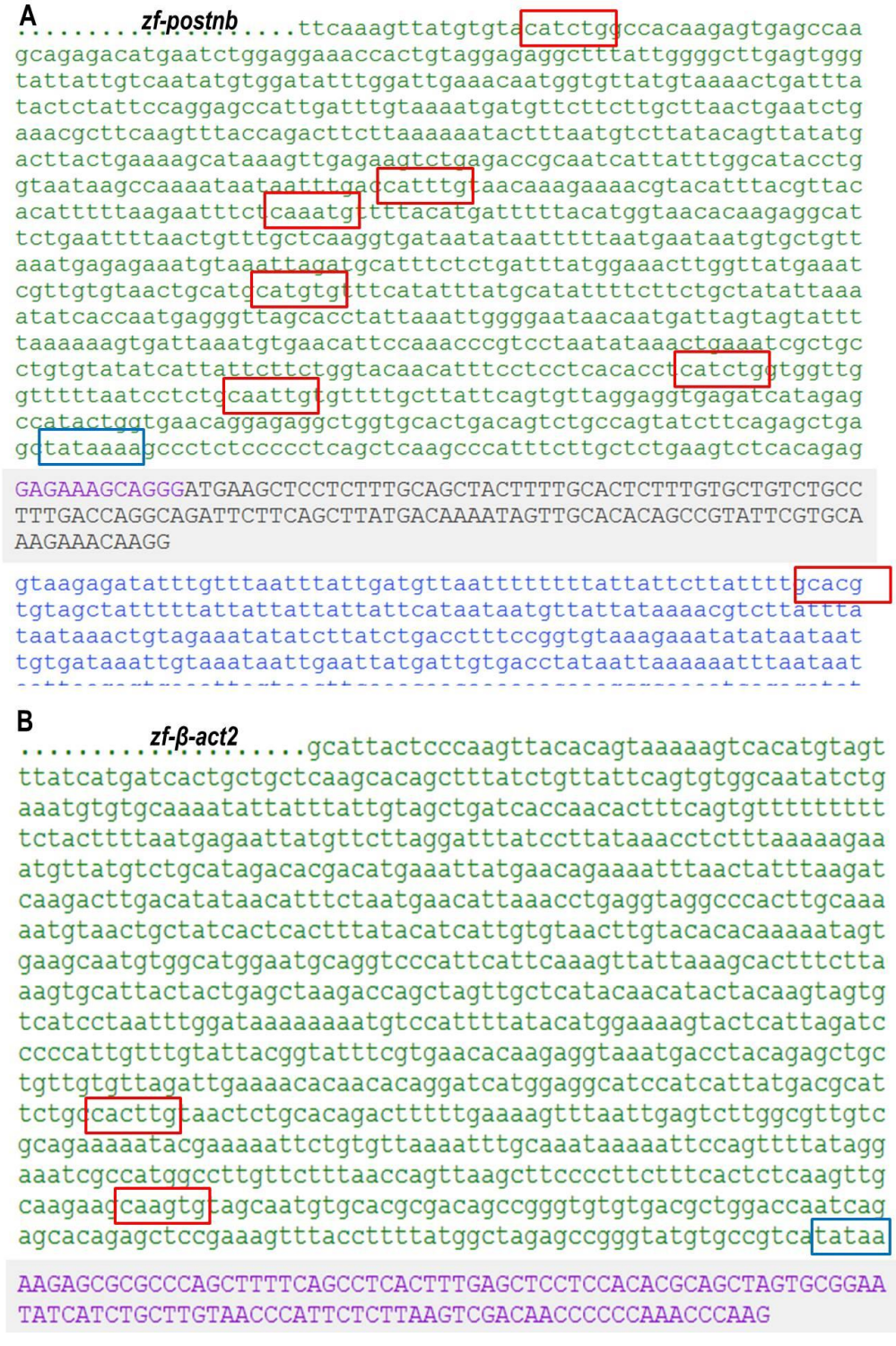

Figure 31: *twist* Binding Sites in *postnb* and *β-act2* Promoter

(A-B) 1 kb upstream regulatory sequence of postnb and β-act2 genes are shown with canonical twist binding sites in red boxes, and TATA box in blue. postnb upstream sequence contains six twist binding sites (and one more in the first intron), and β-act2 two. These two gene were used for

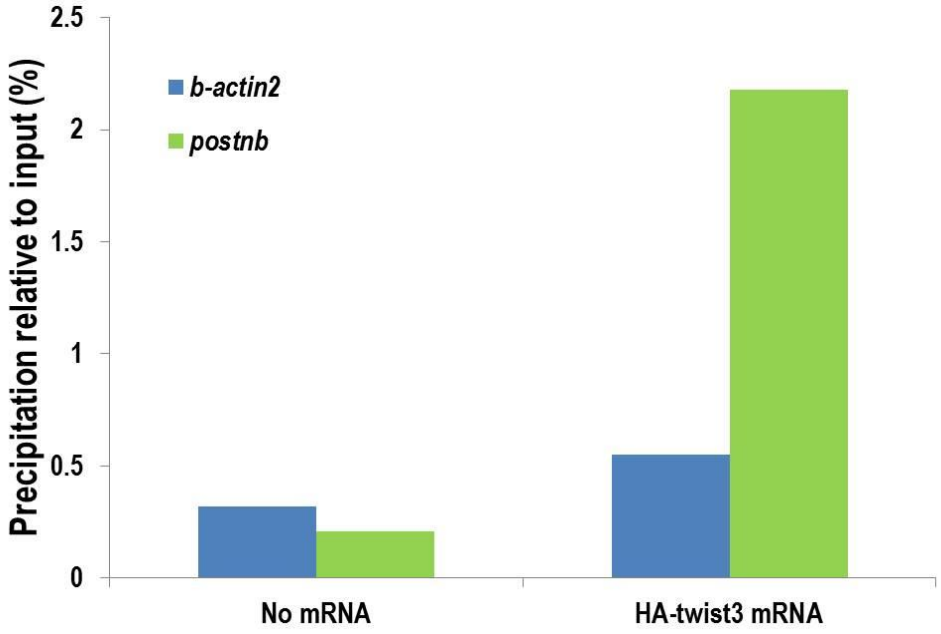

Figure 32: *HA-twist3* ChiP shows Enrichment for *postnb* Promoter

Embryos injected with *HA-twist3* mRNA were collected at 24 hpf and analyzed for pulldown of gene promoters using antibody against HA epitope. Real-time PCR analysis suggested significant enrichment of *postnb* gene regulatory sequences as compared to *β-act2* sequences, suggesting binding of *twist3* gene to *postnb* promoter.

4.9 Summary of Future Work

The following experiments need to be conducted in the short-term to validate the contribution from non-osteoblasts towards bone regeneration and the molecular working model:

1. Multi-color clonal analysis of mesenchymal (fibroblast + osteoblast) compartment development and regeneration
2. Analysis of *twist3* null mutant
3. Generation and analysis of *fgfr4* null mutant
4. ChiP Analysis for *HA-twist3* from adult fins
5. Analyze HA-twist3 expression in female reproductive system

References

Akimenko, M.A., S.L. Johnson, M. Westerfield, and M. Ekker. 1995. Differential induction of four msx homeobox genes during fin development and regeneration in zebrafish. *Development*. 121:347–357.

Akimenko, M.A., M. Mari-Beffa, J. Becerra, and J. Geraudie. 2003. Old questions, new tools, and some answers to the mystery of fin regeneration. *Developmental Dynamics.* 226:190-201.

Alison, M.R., M. Golding, C.E. Sarraf, R.J. Edwards, and E.N. Lalani. 1996. Liver damage in the rat induces hepatocyte stem cells from biliary epithelial cells. *Gastroenterology*. 110:1182-1190.

Apte, S.S., M.F. Seldin, M. Hayashi, and B.R. Olsen. 1992. Cloning of the human and mouse type X collagen genes and mapping of the mouse type X collagen gene to chromosome 10. *European Journal of Biochemistry*. 206:217-224.

Bedell, V.M., Y. Wang, J.M. Campbell, T.L. Poshusta, C.G. Starker, R.G. Krug, 2nd, W. Tan, S.G. Penheiter, A.C. Ma, A.Y. Leung, S.C. Fahrenkrug, D.F. Carlson, D.F. Voytas, K.J. Clark, J.J. Essner, and S.C. Ekker. 2012. In vivo genome editing using a high-efficiency TALEN system. *Nature*. 491:114-118.

Bialek, P., B. Kern, X. Yang, M. Schrock, D. Sosic, N. Hong, H. Wu, K. Yu, D.M. Ornitz, E.N. Olson, M.J. Justice, and G. Karsenty. 2004. A Twist Code Determines the Onset of Osteoblast Differentiation. *Developmental Cell*. 6:423-435.

Carlson, D.F., W. Tan, S.G. Lillico, D. Stverakova, C. Proudfoot, M. Christian, D.F. Voytas, C.R. Long, C.B. Whitelaw, and S.C. Fahrenkrug. 2012. Efficient TALEN-mediated gene knockout in livestock. *Proceedings of the National Academy of Sciences of the United States of America*. 109:17382-17387.

Cermak, T., E.L. Doyle, M. Christian, L. Wang, Y. Zhang, C. Schmidt, J.A. Baller, N.V. Somia, A.J. Bogdanove, and D.F. Voytas. 2011a. Efficient design and assembly of custom TALEN and other TAL effector-based constructs for DNA targeting. *Nucleic Acids Research*. 39:e82.

Cermak, T., E.L. Doyle, M. Christian, L. Wang, Y. Zhang, C. Schmidt, J.A. Baller, N.V. Somia, A.J. Bogdanove, and D.F. Voytas. 2011b. Efficient design and assembly of

custom TALEN and other TAL effector-based constructs for DNA targeting. *Nucleic Acids Research*. 39:e82.

Cobiella, C., F. Haddad, and I. Bacaresce-Hamilton. 1997. Phalangealo metaplasia following amputation in a child's finger. *Injury*. 28:409-410.

Curado, S., R.M. Anderson, B. Jungblut, J. Mumm, E. Schroeter, and D.Y. Stainier. 2007. Conditional targeted cell ablation in zebrafish: a new tool for regeneration studies. *Developmental Dynamics.* 236:1025-1035.

Dahlem, T.J., K. Hoshijima, M.J. Jurynec, D. Gunther, C.G. Starker, A.S. Locke, A.M. Weis, D.F. Voytas, and D.J. Grunwald. 2012. Simple methods for generating and detecting locus-specific mutations induced with TALENs in the zebrafish genome. *PLoS Genet*. 8:e1002861.

Dinsmore, C.E. 1991. A history of regeneration research: milestones in the evolution of a science. Cambridge University Press.

Dor, Y., J. Brown, O.I. Martinez, and D.A. Melton. 2004. Adult pancreatic beta-cells are formed by self-duplication rather than stem-cell differentiation. *Nature*. 429:41-46.

Dunis, D.A., and M. Namenwirth. 1977. The role of grafted skin in the regeneration of x-irradiated axolotl limbs. *Developmental Biology*. 56:97-109.

Gaj, T., C.A. Gersbach, and C.F. Barbas III. 2013. ZFN, TALEN, and CRISPR/Cas-based methods for genome engineering. *Trends in Biotechnology*.

Gemberling, M., T.J. Bailey, D.R. Hyde, and K.D. Poss. 2013. The zebrafish as a model for complex tissue regeneration. *Trends in Genetics*.

Goss, R.J., and M.W. Stagg. 1957. The regeneration of fins and fin rays in Fundulus heteroclitus. *Journal of Experimental Zoology*. 136:487–507.

Goujon, M., H. McWilliam, W. Li, F. Valentin, S. Squizzato, J. Paern, and R. Lopez. 2010. A new bioinformatics analysis tools framework at EMBL–EBI. *Nucleic Acids Research*. 38:W695-W699.

Grohmann, M., N. Paulmann, S. Fleischhauer, J. Vowinckel, J. Priller, and D.J. Walther. 2009. A mammalianized synthetic nitroreductase gene for high-level expression. *BMC Cancer*. 9:301.

Gupta, V., M. Gemberling, R. Karra, Gabriel E. Rosenfeld, T. Evans, and Kenneth D. Poss. 2013. An Injury-Responsive Gata4 Program Shapes the Zebrafish Cardiac Ventricle. *Current Biology : CB*. 23:1221-1227.

Gupta, V., and K.D. Poss. 2012. Clonally dominant cardiomyocytes direct heart morphogenesis. *Nature*. 484:479-484.

Hornik, C., B. Brand-Saberi, S. Rudloff, B. Christ, and E.-M. Füchtbauer. 2004. Twist is an integrator of SHH, FGF, and BMP signaling. *Anatomy and Embryology*. 209:31-39.

Hwang, W.Y., Y. Fu, D. Reyon, M.L. Maeder, S.Q. Tsai, J.D. Sander, R.T. Peterson, J.R. Yeh, and J.K. Joung. 2013. Efficient genome editing in zebrafish using a CRISPR-Cas system. *Nature Biotechnology*. 31:227-229.

Hyde, D.R., A.R. Godwin, and R. Thummel. 2012. In vivo Electroporation of Morpholinos into the Regenerating Adult Zebrafish Tail Fin.e3632.

Inohaya, K., Y. Takano, and A. Kudo. 2007. The teleost intervertebral region acts as a growth center of the centrum: in vivo visualization of osteoblasts and their progenitors in transgenic fish. *Developmental Dynamics.* 236:3031-3046.

Iovine, M.K. 2007. Conserved mechanisms regulate outgrowth in zebrafish fins. *Nature Chemical Biology*. 3:613-618.

Karsenty, G. 2008. Transcriptional control of skeletogenesis. *Annual Review of Genomics and Human Genetics*. 9:183-196.

Karsenty, G., H.M. Kronenberg, and C. Settembre. 2009. Genetic control of bone formation. *Annual Review of Cell and Developmental Biology*. 25:629-648.

Kikuchi, K., J.E. Holdway, A.A. Werdich, R.M. Anderson, Y. Fang, G.F. Egnaczyk, T. Evans, C.A. Macrae, D.Y. Stainier, and K.D. Poss. 2010. Primary contribution to zebrafish heart regeneration by gata4(+) cardiomyocytes. *Nature*. 464:601-605.

Knopf, F., C. Hammond, A. Chekuru, T. Kurth, S. Hans, C.W. Weber, G. Mahatma, S. Fisher, M. Brand, S. Schulte-Merker, and G. Weidinger. 2011. Bone regenerates

via dedifferentiation of osteoblasts in the zebrafish fin. *Developmental Cell*. 20:713-724.

Komaki, M., T. Karakida, M. Abe, S. Oida, K. Mimori, K. Iwasaki, K. Noguchi, S. Oda, and I. Ishikawa. 2007. Twist negatively regulates osteoblastic differentiation in human periodontal ligament cells. *Journal of Cellular Biochemistry*. 100:303-314.

Kragl, M., D. Knapp, E. Nacu, S. Khattak, M. Maden, H.H. Epperlein, and E.M. Tanaka. 2009. Cells keep a memory of their tissue origin during axolotl limb regeneration. *Nature*. 460:60-65.

Krawchuk, D., S.J. Weiner, Y.T. Chen, B.C. Lu, F. Costantini, R.R. Behringer, and E. Laufer. 2010. Twist1 activity thresholds define multiple functions in limb development. *Developmental Biology*. 347:133-146.

Kronenberg, H.M. 2004. Twist Genes Regulate Runx2 and Bone Formation. *Developmental Cell*. 6:317-318.

Larkin, M.A., G. Blackshields, N.P. Brown, R. Chenna, P.A. McGettigan, H. McWilliam, F. Valentin, I.M. Wallace, A. Wilm, R. Lopez, J.D. Thompson, T.J. Gibson, and D.G. Higgins. 2007. Clustal W and Clustal X version 2.0. *Bioinformatics*. 23:2947-2948.

Lee, Y., S. Grill, A. Sanchez, M. Murphy-Ryan, and K.D. Poss. 2005. Fgf signaling instructs position-dependent growth rate during zebrafish fin regeneration. *Development*. 132:5173-5183.

Lee, Y., D. Hami, S. De Val, B. Kagermeier-Schenk, A.A. Wills, B.L. Black, G. Weidinger, and K.D. Poss. 2009a. Maintenance of blastemal proliferation by functionally diverse epidermis in regenerating zebrafish fins. *Developmental Biology*. 331:270-280.

Lee, Y., D. Hami, S. De Val, B. Kagermeier-Schenk, A.A. Wills, B.L. Black, G. Weidinger, and K.D. Poss. 2009b. Maintenance of blastemal proliferation by functionally diverse epidermis in regenerating zebrafish fins. *Developmental biology*. 331:270-280.

Lee, Y., G. Nachtrab, P.W. Klinsawat, D. Hami, and K.D. Poss. 2010. Ras controls melanocyte expansion during zebrafish fin stripe regeneration. *Disease Models & Mechanisms*. 3:496-503.

Li, N., K. Felber, P. Elks, P. Croucher, and H.H. Roehl. 2009. Tracking gene expression during zebrafish osteoblast differentiation. *Developmental Dynamics.* 238:459-466.

Lindeman, L.C., L.T. Vogt-Kielland, P. Alestrom, and P. Collas. 2009. Fish'n ChIPs: chromatin immunoprecipitation in the zebrafish embryo. *Methods in Molecular Biology*. 567:75-86.

Liu, S.Y., C. Selck, B. Friedrich, R. Lutz, M. Vila-Farre, A. Dahl, H. Brandl, N. Lakshmanaperumal, I. Henry, and J.C. Rink. 2013. Reactivating head regrowth in a regeneration-deficient planarian species. *Nature*. 500:81-84.

Livet, J., T.A. Weissman, H. Kang, R.W. Draft, J. Lu, R.A. Bennis, J.R. Sanes, and J.W. Lichtman. 2007. Transgenic strategies for combinatorial expression of fluorescent proteins in the nervous system. *Nature*. 450:56-62.

Lo, D.C., F. Allen, and J.P. Brockes. 1993. Reversal of muscle differentiation during urodele limb regeneration. *Proceedings of the National Academy of Sciences*. 90:7230-7234.

Loebel, D.A., A.C. Hor, H. Bildsoe, V. Jones, Y.T. Chen, R.R. Behringer, and P.P. Tam. 2012. Regionalized Twist1 activity in the forelimb bud drives the morphogenesis of the proximal and preaxial skeleton. *Developmental Biology*. 362:132-140.

Mali, P., L. Yang, K.M. Esvelt, J. Aach, M. Guell, J.E. DiCarlo, J.E. Norville, and G.M. Church. 2013. RNA-guided human genome engineering via Cas9. *Science*. 339:823-826.

Martin, G.R. 1998. The roles of FGFs in the early development of vertebrate limbs. *Genes & development*. 12:1571-1586.

McKim, L.H. 1932. Regeneration of the distal phalanx. *Canadian Medical Association Journal*. 26:549.

Morcos, P.A., Y. Li, and S. Jiang. 2008. Vivo-Morpholinos: a non-peptide transporter delivers Morpholinos into a wide array of mouse tissues. *Biotechniques*. 45:613-614.

Morrison, J.I., S. Lööf, P. He, and A. Simon. 2006. Salamander limb regeneration involves the activation of a multipotent skeletal muscle satellite cell population. *The Journal of cell biology*. 172:433-440.

Nabrit, S.M. 1929. The role of fin rays in the regenreation in the tail-fins of fishes. *The Biological Bulletin*. 56:235–266.

Nabrit, S.M. 1931. The role of the basal plate in regeneration in the tail-fins of fishes. *The Biological Bulletin*. 60:60–63.

Namenwirth, M. 1974. The inheritance of cell differentiation during limb regeneration in the axolotl. *Developmental Biology*. 41:42-56.

Nechiporuk, A., and M.T. Keating. 2002. A proliferation gradient between proximal and msxb-expressing distal blastema directs zebrafish fin regeneration. *Development*. 129:2607-2617.

Niswander, L., C. Tickle, A. Vogel, I. Booth, and G.R. Martin. 1993. FGF-4 replaces the apical ectodermal ridge and directs outgrowth and patterning of the limb. *Cell*. 75:579-587.

O'Rourke, M.P., K. Soo, R.R. Behringer, C.-C. Hui, and P.P. Tam. 2002. Twist Plays an Essential Role in FGF and SHH Signal Transduction during Mouse Limb Development. *Developmental Biology*. 248:143-156.

O Rourke, M.P., and P.P. Tam. 2002. Twist functions in mouse development. *International Journal of Developmental Biology*. 46:401-414.

Oshima, A., H. Tanabe, T. Yan, G.N. Lowe, C.A. Glackin, and A. Kudo. 2002. A novel mechanism for the regulation of osteoblast differentiation: transcription of periostin, a member of the fasciclin I family, is regulated by the bHLH transcription factor, twist. *Journal of Cellular Biochemistry*. 86:792-804.

Ozdemir, A., K.I. Fisher-Aylor, S. Pepke, M. Samanta, L. Dunipace, K. McCue, L. Zeng, N. Ogawa, B.J. Wold, and A. Stathopoulos. 2011. High resolution mapping of Twist to DNA in Drosophila embryos: Efficient functional analysis and evolutionary conservation. *Genome Research*. 21:566-577.

Poss, K.D. 2010. Advances in understanding tissue regenerative capacity and mechanisms in animals. *Nature Reviews. Genetics*. 11:710-722.

Poss, K.D., M.T. Keating, and A. Nechiporuk. 2003. Tales of regeneration in zebrafish. *Developmental Dynamics.* 226:202-210.

Poss, K.D., L.G. Wilson, and M.T. Keating. 2002. Heart regeneration in zebrafish. *Science*. 298:2188-2190.

Ran, F., P.D. Hsu, C.-Y. Lin, J.S. Gootenberg, S. Konermann, A.E. Trevino, D.A. Scott, A. Inoue, S. Matoba, and Y. Zhang. 2013. Double Nicking by RNA-Guided CRISPR Cas9 for Enhanced Genome Editing Specificity. *Cell*.

Renn, J., and C. Winkler. 2009. Osterix-mCherry transgenic medaka for in vivo imaging of bone formation. *Developmental Dynamics.* 238:241-248.

Sikes, J.M., and P.A. Newmark. 2013. Restoration of anterior regeneration in a planarian with limited regenerative ability. *Nature*. 500:77-80.

Singh, S., and A.O. Gramolini. 2009. Characterization of sequences in human TWIST required for nuclear localization. *BMC cell biology*. 10:47.

Sousa, S., N. Afonso, A. Bensimon-Brito, M. Fonseca, M. Simoes, J. Leon, H. Roehl, M.L. Cancela, and A. Jacinto. 2011. Differentiated skeletal cells contribute to blastema formation during zebrafish fin regeneration. *Development*. 138:3897-3905.

Steen, T.P. 1968. Stability of chondrocyte differentiation and contribution of muscle to cartilage during limb regeneration in the axolotl (Siredon mexicanum). *Journal of Experimental Zoology*. 167:49-77.

Steen, T.P. 1970. Origin and Differentiative Capacities of Cells in the Blastema of the Regenerating Salamander Limb. *American Zoologist*. 10:119-132.

Stewart, S., and K. Stankunas. 2012. Limited dedifferentiation provides replacement tissue during zebrafish fin regeneration. *Developmental Biology*. 365:339-349.

Subach, O.M., I.S. Gundorov, M. Yoshimura, F.V. Subach, J. Zhang, D. Grüenwald, E.A. Souslova, D.M. Chudakov, and V.V. Verkhusha. 2008. Conversion of Red Fluorescent Protein into a Bright Blue Probe. *Chemistry & biology*. 15:1116-1124.

Sun, X., F.V. Mariani, and G.R. Martin. 2002. Functions of FGF signalling from the apical ectodermal ridge in limb development. *Nature*. 418:501-508.

Tanaka, E.M., and P.W. Reddien. 2011. The cellular basis for animal regeneration. *Developmental cell*. 21:172–185.

Thorel, F., V. Nepote, I. Avril, K. Kohno, R. Desgraz, S. Chera, and P.L. Herrera. 2010. Conversion of adult pancreatic alpha-cells to beta-cells after extreme beta-cell loss. *Nature*. 464:1149-1154.

Thornton, C.S. 1938. The histogenesis of the regenerating fore limb of larval Amblystoma after exarticulation of the humerus. *Journal of Morphology*. 62:219–241.

Trichas, G., J. Begbie, and S. Srinivas. 2008. Use of the viral 2A peptide for bicistronic expression in transgenic mice. *BMC biology*. 6:40.

Tu, S., and S.L. Johnson. 2011. Fate restriction in the growing and regenerating zebrafish fin. *Developmental cell*. 20:725-732.

Turner, C.J. 1941. Regeneration of the gonopodium of Gambusia during morphogenesis. *Journal of Experimental Zoology*. 87:181–210.

Umesono, Y., J. Tasaki, Y. Nishimura, M. Hrouda, E. Kawaguchi, S. Yazawa, O. Nishimura, K. Hosoda, T. Inoue, and K. Agata. 2013. The molecular logic for planarian regeneration along the anterior-posterior axis. *Nature*. 500:73-76.

Vidal, P., and M. Dickson. 1993. Regeneration of the distal phalanx: a case report. *The Journal of Hand Surgery: British & European Volume*. 18:230-233.

Vogel, A., C. Rodriguez, and J.-C. Izpisúa-Belmonte. 1996. Involvement of FGF-8 in initiation, outgrowth and patterning of the vertebrate limb. *Development*. 122:1737-1750.

Whitehead, G.G. 2005. fgf20 Is Essential for Initiating Zebrafish Fin Regeneration. *Science*. 310:1957-1960.

Wills, A.A., A.R. Kidd, A. Lepilina, and K.D. Poss. 2008. Fgfs control homeostatic regeneration in adult zebrafish fins. *Development*. 135:3063-3070.

Yang, D.-C., C.-C. Tsai, Y.-F. Liao, H.-C. Fu, H.-J. Tsay, T.-F. Huang, Y.-H. Chen, and S.-C. Hung. 2011. Twist Controls Skeletal Development and Dorsoventral Patterning by Regulating *Runx2* in Zebrafish. *PLoS ONE*. 6:e27324.

Yin, V.P., and K.D. Poss. 2008. New regulators of vertebrate appendage regeneration. *Current opinion in genetics & development*. 18:381-386.

Zeitlinger, J., R.P. Zinzen, A. Stark, M. Kellis, H. Zhang, R.A. Young, and M. Levine. 2007. Whole-genome ChIP-chip analysis of Dorsal, Twist, and Snail suggests integration of diverse patterning processes in the Drosophila embryo. *Genes & development*. 21:385-390.

Biography

Sumeet P. Singh was born August 12, 1985 in Kanpur, UP, India. He attended Holy Cross English High School in Aurangabad till 2001, and then Bhavans College in Mumbai from 2001-03.

He cleared Indian Institute of Technology (IIT) Joint Entrance Exam (JEE) in 2004 and attended IIT-Kanpur for undergraduate studies in BioEngineering, graduating with Bachelors in 2008.

He started graduate school at Duke University in Durham, US and joined the Poss Lab working on zebrafish regeneration in December, 2008. During his graduate work, Sumeet published a Developmental Cell article on work in fin regeneration.